A cross-layer cooperation strategy for cellular networks.

Su, Geng

A cross-layer cooperation strategy for cellular networks

Geng Su

Submitted for the degree of Doctor of Philosophy

School of Electronic Engineering and Computer Science

Queen Mary, University of London

September 2012

Dedicated to whom I love

Abstract

Cooperation is seen as a means to improve the signal in OFDMA wireless networks by overcoming the inter-cell interference. Such co-operation can be deployed in both the physical layer and the MAC layer. In this thesis, a cross-layer cooperation strategy is considered.

Firstly, in the physical layer, a cooperative coding scheme with private information sharing is proposed based on dirty paper coding; this is analyzed in a scenario with two transmitters and two receivers. To implement the cooperation, a rate limited link is deployed at the transmitters' side in order to share the information. A new achievable rate region is established in both strong interference regime and weak interference regime.

Secondly, in the MAC layer, a graph-based dynamic coordinated clustering scheme is proposed. An interference weighted graph is constructed to assist dynamic coordinated clustering for inter-cell interference mitigation and to improve the cell-edge user performance. Only 2 bits are allowed for the signalling exchange between transmitters and this reduces the overhead of the approach. The system throughput and cell-edge throughput with different user distributions are used to evaluate the performance.

Thirdly, a transmit antenna selection algorithm is presented to optimize system performance with the constraint of fairness. A graph is generated by using the channel condition between the transmit antennas and Mobile Stations. Based on the graph, a heuristic algorithm is proposed to choose the transmit antenna for each user in order to improve the system performance and guarantee the user fairness.

Finally, combining the cooperative coding scheme and cooperative clustering scheme, a cross-layer cooperation scheme is presented. In the physical layer, the cooperation

coding scheme mitigates the interference and increases the transmission rate; in the MAC layer, the cooperative clustering scheme provides efficient cooperative transmission. Simulation results show that the proposed scheme can effectively increase both the system throughput and cell-edge throughput.

Acknowledgment

This thesis arose in the past year of research that has been done since I came to Queen Mary, University of London, I have worked with a large number of people whose contribution in assorted ways to the research and the making of the thesis deserved special mention. It is a pleasure to convey my gratitude to them all in my humble acknowledgment.

In the first place I would like to record my gratitude to my supervisor Professor Laurie Cuthbert for his advice, supervision, and contribution. His involvement with his originality has triggered and nourished my intellectual maturity that I will benefit from, for a long time to come. He gave me lots of freedom to undertake research, and never criticized me directly but encouraged me on every small progress.

I gratefully acknowledge Dr Yue Chen and Dr Frank Gao for their valuable advice in scientific discussions and spending their time answering questions, even some unintelligent ones from me about cooperation technique.

I also benefited by outstanding works from QMUL colleagues. My thanks go to Lin Xiao, Dapeng Zhang, Hongyi Xiong, Lexi Xu, Ling Xu, Fei Peng, Kashif, Ammar, and so many others. You are my best friends forever.

Thanks also to my family with their inseparable support and help.

Finally, I would like to thank everybody who has ever helped me. With my love and gratitude, I want to dedicate this thesis to all the people I love.

Contents

List of Figures

List of Tables

List of Abbreviations

B3G	beyond 3rd generation
BBU	base band unit
BS	base station
BSC	base station cooperation
CDF	cumulative distribution function
CDMA	code division multiple access
CQI	channel quality information
D-MIMO	distributed multiple input multiple output
DL	downlink
eNB	evolve nodeB
FDMA	frequency division multiple access
GBTS	graph based transmit antenna selection
GBTS-F	graph based transmit antenna selection with fairness
GBDCS	graph based dynamic clustering selection
IC	interference channel
ICI	inter cell interference
ICIC	inter cell interference coordination
LB	load balance
LTE	long term evolution
LTE-A	long term evolution advance
MAC	multiple access control
MME/GW	mobility management entity/gateway
MIMO	multiple input multiple output

MU-MIMO	multi user multiple input multiple output
MS	mobile station[1]
NGN	next generation network
OFDM	orthogonal frequency division multiplexing
OFDMA	orthogonal frequency division multiplexing access
PF	proportional fairness
QoS	quality of service
PHY	physical layer
PRB	physical resource block
RB	resource block
RRM	radio resource management
RRU	remote radio unit
RS	relay station
SNR	signal to noise ratio
SINR	signal to interference and noise ratio
SVD	singular value decomposition
SU-MIMO	single user multiple input multiple output
SCM	spatial channel module
SCME	spatial channel module evolve
TDMA	time division multiple access
TTI	transmit time interval
UL	uplink

[1] UE (User Equipment) is used by 3GPP to denote the mobile station, but for consistency MS is used throughout this thesis.

Notation

$\mathbb{C}$	In PHY: set of complex numbers
	In MAC: cooperative set
$\mathbb{R}$	Set of real number
$\mathbb{E}(x)$	Expected value of random variable x
$H^{(t)}$	Channel matrix
N	MIMO channel: number of transmit antenna
	Cellular system: number of antenna per base
M	MIMO channel: number of receive antenna
	Cellular system: number of antenna per user
x	Received signal vector
G,g	Precoding matrix, vector
$diagA$	Diagonal elements of square matrix A
trA	Trace of square matrix A
I_N	$N \times N$ identity matrix
Z	Shadow fading realization
G	Directional antenna response
γ	In PHY: Shannon capacity
	In MAC: SINR
α, β	Power allocation parameter
δ^2	Noise variance
$\mathcal{E}$	edge in graph
P	Signal power

P/δ^2	SU-MIMO and MU-MIMO channel: average SNR
	Cellular system: reference SNR
Q	Time variable
R	Achievable rate region

1. Introduction

1.1. Research scope

Next generation networks (NGN) aim to give a total cell capacity of up to 1Gbps for slow-moving users and 100Mbps for fast moving users. Technologies such as multiple input multiple output (MIMO) and orthogonal frequency division multiplexing access (OFDMA) will be used in NGN to allow this performance to be achieved. By using OFDMA, there will be no intra-cell interference but as there will be channel reuse in a multi-cell environment, it is inevitable that there will be co-channel interference from other cells. Therefore, inter-cell interference is seen as the bottleneck that limits the system performance [1]

Mitigating the inter-cell interference has become a severe problem. A simple idea is to avoid the interference so that many researchers have considered techniques such as spectrum reuse [1][2][3] and smart antennas [4][5][6]. Cooperation is now seen as an important technology [7][8][9]: this lets several transmitters transmit the signal or allocates radio resources by jointly mitigating the inter-cell interference and increasing the desired signal strength.

Introducing cooperation into conventional cellular networks brings new research considerations to decide:

- whether to operate with cooperative coding or not;
- which users will be selected as cooperation users;
- which BSs will be selected to transmit the signal to users; and
- how many BSs can form a cooperation set.

This thesis describes research into cooperation in cellular networks. The goal of the research is to determine fairness, throughput and the size of cooperation set in cellular network in order to find an efficient way to allocate the resources to achieve the optimal solution.

Base station cooperation can convert the interference channel into the desired signal channel, which will improve the system throughput. The first step is to form it potential cooperative set (also known as the *diversity set*); the second is to design an appropriate algorithm to form the cooperative set for each user from the diversity set. After that, a cooperative coding scheme would be used to provide cooperative transmission.

Resource block (RB) allocation is another important issue for system performance and resource efficiency. Determining how RBs will be allocated between cooperative and non-cooperative users and how to avoid conflicting RB allocation in cooperative cellular networks is important to enhance the system performance.

1.2. Research Contribution

The work reported in this thesis is novel. The main contributions are as follow:

1. Transmit antenna selection

This thesis proposes a transmit-antenna selection algorithm for a distributed-MIMO (D-MIMO) system to obtain the spatial multiplexing and mitigate the inter-cell interference (ICI). Each user will choose its own transmit antenna depending on the channel condition with a fairness constraint (an extension of the concept of proportional fairness) being taken into consideration in the selection algorithm.

2. Cooperation set selection

A base station cooperation selection algorithm is proposed to design the cooperation set for each user to improve the system throughput and mitigate inter-cell interference. A quantized value is generated according to the position of the mobile station (MS) and its potential cooperation set. The quantized value will construct the users' weight in all cells. A max matching and assignment algorithm is used to form the cooperative set for each user according to the users' weight.

3. Radio resource allocation in cooperation cellular scenario.

A radio resource allocation algorithm is proposed to allocate RBs to each user in a cooperative cellular network in order to avoid conflicting RB allocation.

1.3. Author's Publications

[1] Tiankui Zhang; Chunyan Feng; Geng Su; Lin Xiao, "Uplink Multi-Cell Non-Cooperative Power Allocation Game Algorithm for OFDMA Cellular Networks," *Wireless Communications, Networking and Mobile Computing, 2009. WiCom '09. 5th International Conference* on, vol., no., pp.1-4, 24-26 Sept. 2009

[2] Geng Su; Cuthbert, Laurie; Tiankui Zhang; , "A graph-based dynamic coordinated clustering scheme for base station cooperation," *Communication Technology and Application (ICCTA 2011), IET International Conference on*, vol., no., pp.201-206, 14-16 Oct. 2011

[3] Lin Xiao; Tiankui Zhang; Cuthbert, L.; Geng Su; , "Scheduling Algorithm for Multimedia Services in Relay Based OFDMA Cellular Networks," *Wireless Communications and Mobile Computing Conference (IWCMC)*, 2011 7th International , vol., no., pp.1900-1905, 4-8 July 2011

1.4. Thesis Organization

The remainder of this thesis is organized as follows

Chapter 2 briefly describes the architecture of the next generation mobile network: Long Term Evolution (LTE); it also introduces the relevant concepts in cooperation, including basic principles, capacity limitation and the use of cooperation. A simple introduction of multiple antenna technology in LTE networks is also given.

Chapter 3 discusses the simulator used for this research on cooperative cellular networks. The overall design of the simulation platform and the main function procedures, together with the choice of parameters, are described in this chapter.

Validation is an important aspect of any simulator implementation and this is considered in the last part of this chapter.

Chapter 4 reports the research on the transmit antenna selection in a MIMO system. A multi-cell cooperation transmit antenna selection algorithm (based on game theory) for throughput with fairness constraints is proposed and the performance discussed.

Chapter 5 investigates the cooperation-set selection algorithm in a base-station cooperation network. The assisted graph is constructed based on optimal assignment of graph theory and the RB allocation scheme is described; the simulation results are used to evaluate the performance.

Chapter 6 proposes a new cooperative coding scheme in a two-transmitter, two-receiver interference channel model. To implement the cooperation, a rate limited link is deployed at the transmitter side in order to share the information. A new coding scheme with private information sharing is proposed based on the dirty paper coding scheme. A new achievable rate region is established in order to evaluate the performance theoretically.

Chapter 7 gives the system performance evaluation of the proposed cross-layer cooperative transmission scheme.

Chapter 8 concludes the works in this thesis, and discussed the potential direction of the future work

2. Cooperative based LTE Networks

2.1. Introduction to LTE Networks

Higher data rate and higher quality mobile communication services are permanent demands for Mobile users. High-speed packet access (HSPA) in 3G can provides up to 2Mbps, but in order to meet the continued traffic growth demands, the 3G Partnership Project (3GPP) developed a new standard for the evolution of GSM/HSPA technology towards a higher data rate system referred to as Long-Term Evolution (LTE).

The LTE standard aims to create specifications for a new radio-access technology geared to higher data rates, low latency and high spectral efficiency [10]. The spectral efficiency for LTE system is three to four times higher than the current HSPA system [11]. To meet such high spectral efficiency requirement, LTE system deploys many advanced techniques such as *multiple-input multiple-output* (MIMO) techniques, *Orthogonal Frequency Division Multiple Access* (OFDMA) techniques, inter-cell interference mitigation techniques.

As mentioned above, OFDMA is the access technology used for LTE network [12]. By allocating frequency resource orthogonally, intra-cell interference is eliminated but inter-cell interference now becomes the limiting factor. Therefore, to achieve the high data-rates required, cooperation between the neighbouring cell and *Mobile station* (MS, also known as User Equipment, UE,) is being more intensively studied [4]. One important focus of these studies is to increase the data throughput for the cell-edge MS by using cooperation between neighbouring eNBs (base stations) to enhance the signal quality and /or decrease the interference level [13][14][15]. Coverage extension through a wireless relay is another research focus of cooperative communication [8]. *Multiple Input Multiple Output* (MIMO) technology is used to improve transmission performance and this is considered in more detail in 2.4.

2.1.1. Introduction of the network architecture in LTE Networks

LTE is designed to support packet-switched traffic with seamless mobility, QoS and minimal latency and to do this it uses a highly simplified flat architecture with only two types of node (*Evolved Node-B* (eNB) – effectively the base station - and *Mobility Management Entity/Gateway* (MME/GW)).

All the network interfaces are based on IP protocols. The *Evolved Node-B* (eNB) is interconnected by means of an X2 interface and to the *Mobility Management Entity/Gateway* (MME/GW) entity by means of an S1 interfaces as shown in Figure 2.1. The S1 interface supports a many-to-many relationship between MME/GW and eNBs [12].

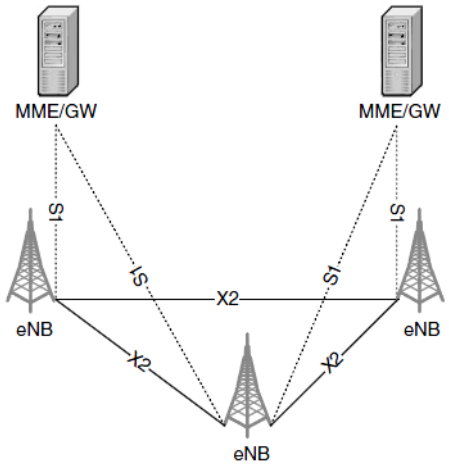

Figure 2.1 Network architecture for LTE [Fig 2.1 from [12]]

The MME is a signalling only entity and hence user IP packets do not go through MME. An advantage of a separate network entity for signalling is that the network capacity for signalling and traffic can grow independently. The main functions of MME are the control and execution of paging, mobility management, roaming, authentication, and authorization.

The eNB implements Node-B functions as well as protocols implemented in the radio

network controller (RNC) in a 3G network. On the control side, eNB incorporates functions such as admission control and radio resource management. Some of the benefits of a single node in the access network are reduced latency and the distribution of RNC processing load across multiple eNBs.

This architecture is in contrast to the use of more network nodes in the hierarchical network architecture of the current 3G system. One major change is that the radio network controller is eliminated from the data path and its functions are now incorporated in the eNB with eNBs communicating directly with each other; this has the benefit of reduced latency as mentioned above.

2.1.2. Introduction of the protocol in LTE

The protocol stack has two planes. Protocols in the *user plane* manage user data, while the protocols in the *control plane* manage the signalling messages.

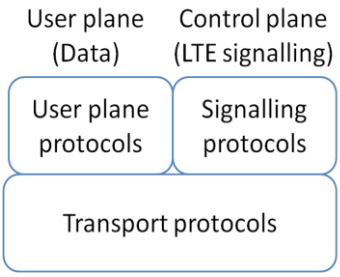

Figure 2.2 High level protocol architecture in LTE (Fig2.9 from [10])

As shown in Figure 2.2, there are then three types of protocol: (i) *signalling protocols* can exchange signalling messages between two devices; (ii) *user plane protocols* control the data in the user plane in order to help route the data within the network; and (iii) the underlying *transport protocols* transfer data and signalling messages from one point to another.

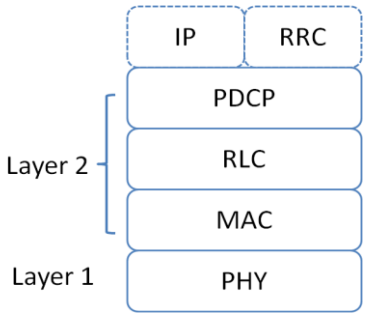

Figure 2.3 Transport protocols used on the air interface (Fig 2.11 from [10])

The air interface lies between the mobile and base station (i.e. between UE and eNB). Figure 2.3 shows the air interface's transport protocols:

- the *physical layer* contains the digital and analogue signal processing functions that the mobile and base station use to send and receive information;
- the *medium access control* (MAC) protocol [16] carries out low-level control of the physical layer, particularly by scheduling data transmissions between the mobile and the base station;
- the *radio link control* (RLC) protocol [17] controls the maintenance of data link between the two devices; and
- the *packet data convergence protocol* (PDCP) [18] carries out higher-level transport functions that are related to header compression and security.

Users require ever higher data rates [19] and the networks have to be designed and deployed with unavoidable constraints on the limited radio resources such as bandwidth and transmit power [20]. Research is therefore needed to improve the capacity and utilization of the radio resources available. In a traditional cellular wireless network, the upper limit of the transmission link is determined by the Shannon capacity [21]. MIMO and cooperative communications have been proposed [22][23] to lead an enhancement in the cell-edge performance of LTE system by effectively improving the channel to get closer to this limit.

2.2. Wireless communication channel

2.2.1. Challenges for wireless communication

There are many severe challenges in wireless radio channel. Due to the user movement and environment changes, the wireless channel not only sensitive to noise, interference, and other channel impediment, but also these impediments change over time in unpredictable ways. There are three main impediments in a wireless communication scenario, as shown Figure 2.4

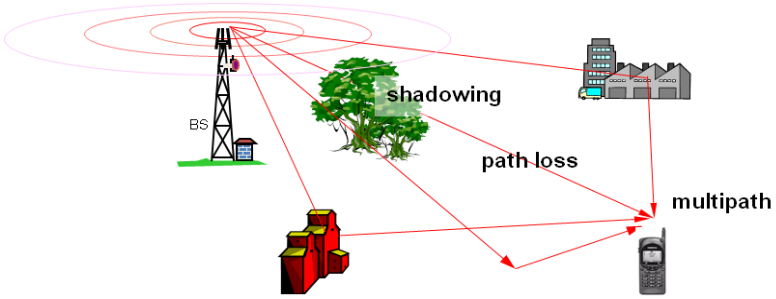

Figure 2.4 Radio transmission impairments

Path-loss is caused by dissipation of the power radiated by the transmitter as well as by effects of the propagation channel.

Shadowing is caused by obstacles between the transmitter and receiver that attenuate signal power through absorption, reflection, scattering, and diffraction. When the attenuation is strong, the signal can be seen as blocked. Since variation in received power due to path-loss and shadowing occur over relatively large distances, these variations are sometimes called as *large-scale fading*.

Multipath fading refers to the signal power variation caused by the constructive and destructive addition of signal components arriving at the receiver through multiple different paths between the transmitter and receiver. These multiple paths are generated by the scattering and reflecting objects located around the transmitter and

receiver.

Multi-path interference may be constructive or destructive depending on the delays on each path and hence the relative phase of the difference components, as shown in Figure 2.5.

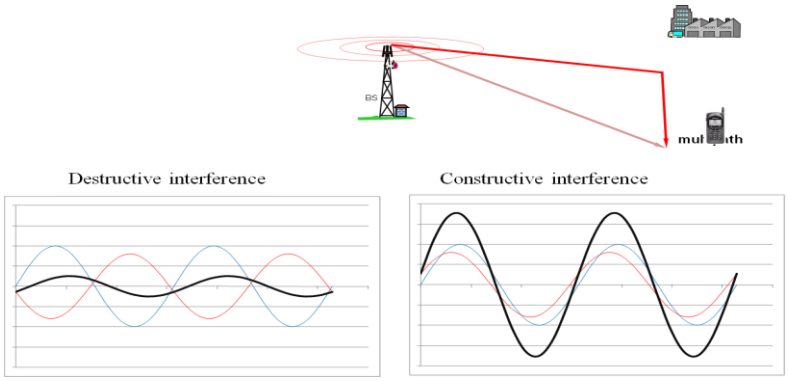

Figure 2.5 interference superposition

2.2.2. Diversity

One of the methods to overcome the unreliability and reinforce the performance of wireless fading channels is to improve the diversity. Diversity techniques mitigate the effect of channel fading by using multiple independent channels. If several replicas of the same information signal are transmitted through independent fading channels, the probability that all the channels undergo deep fading at the same time decreases significantly.

There are several ways to implement the diversity techniques:

- Time diversity, where the same signal is transmitted on different time slots.
- Frequency diversity, where the same signal is transmitted over different subcarriers, with the separation of the carrier frequencies made larger than the coherence bandwidth of the channel.

- Spatial diversity, which achieves the diversity effect by using multiple transmitter and/or receiver antennas.

In an LTE system that has very short subframe transmission time of 1ms, there is not much scope for time-diversity. Therefore, the two main techniques that are used are:

- OFDM, which divides the whole bandwidth into multiple narrow subcarriers, can be used as a frequency diversity technique by associating multiple subcarriers in different frequency regions.

- MIMO, which transmits the information through multiple antennas, thereby increasing the spatial diversity.

2.3. Orthogonal Frequency Division Multiplexing

The 4G LTE system has evolved from the 3G wideband code division multiple access (WCDMA). In WCDMA downlink, different orthogonal codes are transmitted on the same bandwidth. However, in a realistic wireless scenario, due to the multi-path propagation, the codes may no longer be orthogonal and hence will interfere with each other. This multi-path interference can be eliminated by deploying an advanced receiver to overcome this limitation, but at the cost of increasing the complexity.

However, the multi-path interference problem of WCDMA becomes much worse for larger bandwidths, which is exactly the requirement for LTE. Hence OFDMA is used in the LTE downlink.

2.3.1. The principle of OFDM

The basic principle of OFDM is to divide the available spectrum into narrowband parallel channels referred to subcarriers and transmit information on these parallel channels at a reduced signalling rate. The goal is to let each channel experience almost flat-fading simplifying the channel equalization process. The name OFDM comes from the fact that the frequency responses of the subchannels are overlapping

but are orthogonal. This means that channels can be more closely spaced and so it increases the spectral efficiency.

OFDM is, therefore, multi-carrier transmission where data is divided between the different subcarriers of one transmitter. Different subcarriers are orthogonal to each other; i.e. other subcarriers sum to zero for each single subcarrier sampling point.

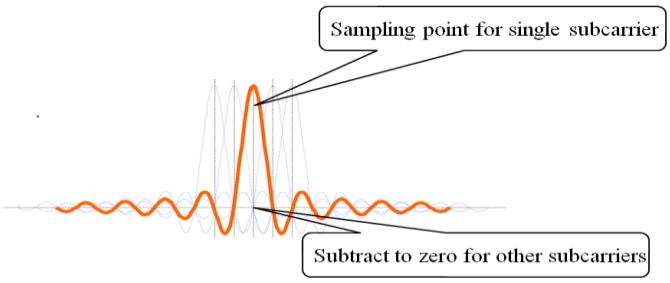

Figure 2.6 orthogonal subcarrier

2.3.2. Advantages of OFDMA

High spectral efficiency: Since the subcarriers partially overlap, the orthogonality preventing interference, there is no guard spectrum needed so OFDM technology can increase the spectral efficiency.

Anti-interference: as OFDM divides the wideband channel into narrowband subcarriers, each subcarrier can be treated as a flat fading channel. Hence, OFDMA avoids frequency-selective fading. Furthermore, since the OFDMA system allocates subcarriers to different users, these users are orthogonal to each other, so the intra-cell interference between users can be eliminated.

Flexible resource allocation: OFDMA allocates subcarriers for transmission according to the channel condition, so dynamic subcarrier allocation is feasible.

2.4. Multiple Input Multiple Output

By deploying OFDM in the cellular network, radio resource is assigned orthogonally

to different users. Therefore, the interference between users in the same cell, also known as **intra**-cell interference, is eliminated. However, users may receive interfering signals from neighbouring cells, so **inter**-cell interference becomes a problem, limiting the system throughput.

Figure 2.7 gives an example to illustrate this problem, showing how edge users suffer worst since the signal from the wanted eNB is weaker for them, while the interfering signal is stronger as they are closer to the interfering eNB.

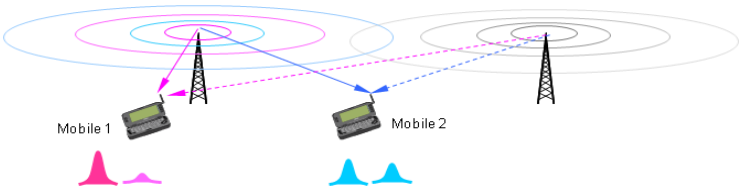

Figure 2.7 example of inter-cell interference

MIMO can be used to overcome this problem [24]: by employing multiple antennas at the transmitter side, receiver side, or both, the robustness (spatial diversity) of a link can be improved as well as the throughput of the link (spatial multiplexing). Depending on the implementation, MIMO techniques can be divided into two parts: single user MIMO and multi user MIMO.

2.4.1. Introduction to MIMO

There is a simple category of multi-antenna types as shown in Table 2.1:

Table 2.1 type of multi-antenna techniques

Multi-antenna types		
SISO	Single-input-single-output means that the transmitter and receiver of the radio system have only one antenna.	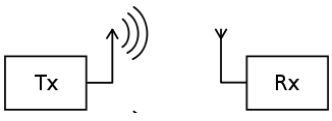

SIMO	Single-input-multiple-output means that the receiver has multiple antennas while the transmitter has one antenna.	
MISO	Multiple-input-single-output means that the transmitter has multiple antennas while the receiver has one antenna.	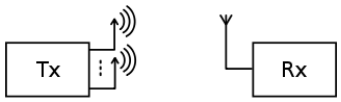
MIMO	Multiple-input-multiple-output means that the both the transmitter and receiver have multiple antennas.	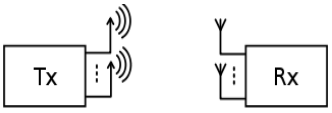

As explained previously, the propagation channel in wireless communication is characterized by multipath propagation that changes with time leading to time-varying fading and SNR variations. With MIMO, the receiving end uses an algorithm to reconstruct the originally transmitted data mitigating the effects of multi-path fading.

MIMO exploits the space dimension to improve wireless systems capacity, range and reliability. It offers significant increases in data throughput and link range without additional bandwidth or increased transmit power. MIMO achieves this goal by spreading the same total transmit power over the antennas to achieve an array gain that improves the spectral efficiency (more bits per second per hertz of bandwidth) or to achieve a diversity gain that improves the link reliability (reduced fading). As the number of antenna elements increases, the channel capacity is increased too.

2.4.2. SU-MIMO

MIMO techniques were first investigated in single-user scenarios. When the data rate is to be increased for a single MS, this is called *Single User MIMO* (SU-MIMO). SU-MIMO is point-to-point multiple antenna transmission as illustrated in Figure 2.8. In a wireless network, deep fading may cause very severe transmission problems,

but utilizing multiple path transmission between the BS and MS, the MIMO system improves the channel gain in order to overcome the fading [25].

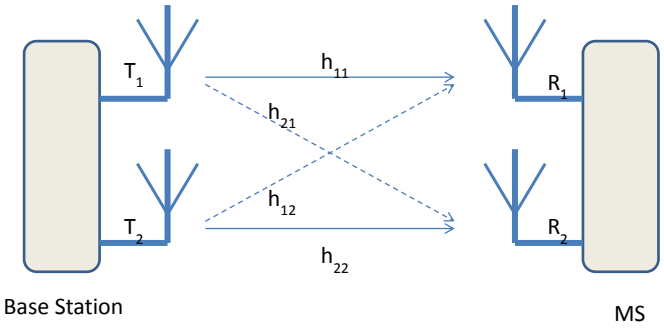

Figure 2.8 Single User MIMO System (Fig 7.1 from [26])

2.4.3. MU-MIMO

When the individual streams are assigned to various users, this is called *Multi User MIMO* (MU-MIMO). In a traditional wireless cellular network, allocating the same spectrum resource to different users would cause severe co-channel interference, but [27][28][29] proposed a coding technique referred to as "writing on dirty paper". In this technique it was shown that the capacity of a channel where the transmitter knows the interfering signal is the same as if there were no interference. For the downlink, the base stations cooperate by simultaneously transmitting to a group of users, as illustrated in Figure 2.9.

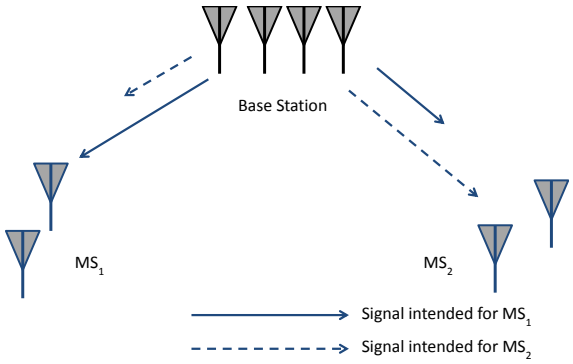

Figure 2.9 Multi User MIMO System [Fig 1 from [28]]

In the situation depicted, the base station attempts to transmit over the same channel to two users, but there is some inter-user interference for user1 generated by the signal transmitted to user2 and vice versa. With some multi user detection methods, it may be possible for a given user to overcome the interference, but such techniques generally cost too much at the receiver. Therefore, it is preferred to mitigate the interference at the transmitter by intelligently designing the transmitted signal. Hence, the channel state information is required.

Due to the inherent characteristic of allocating the same spectrum resources to different users, MU-MIMO provides multiuser diversity with less reliance on antenna diversity and is generally considered better that SU-MIMO [30].

2.4.4. Advantages of MIMO

High spectrum efficiency: since multiple antennas are deployed in the transmitter and receiver sides, multiple parallel signals that are independently and separately encoded, can be transmitted at the same time. Therefore, MIMO techniques can increase the system capacity.

Enhanced system robustness: as the multi-path channels are uncorrelated with each other, the same data signal is transmitted from multiple antennas to improve

the signal-to-noise ratio at the receiver. Therefore, MIMO techniques can improve the system robustness.

2.5. Cooperation

2.5.1. Introduction

The advantages of MIMO have been discussed above and, in principle, MIMO can be implemented by embedding multiple antennas on a device. However, as the size and cost of wireless devices are limited for many applications, which means placing multiple antennas on a single terminal may not be practical. In this case, cooperating with other nodes in the network to form a distributed antenna system is a more realistic alternative. This is achieved by the so-called *cooperative communications.*

Cooperation in wireless networks can take many forms, such as cooperative coding in the physical layer (PHY layer) [31][32], and terminal cooperation in the MAC layer [33][34][35].

Cooperative coding should enhance the diversity and mitigate the interference, but is not always beneficial [36] so that sometimes plain data transmission achieves the same or even better performance. Hence, cooperation and coding schemes have to be dynamically controlled so they are enabled when beneficial but disabled again when the performance is worse than plain transmission.

In the MAC layer there are three kinds of cooperation [37][38][39]:

i) *User Terminal* (UT) cooperation (*Mobile Station* cooperation);
ii) BS cooperation; and
iii) Relaying.

In the PHY layer there is just one:

i) Coding cooperation.

By utilizing a judicious terminal selection scheme in the MAC layer or cooperative

coding scheme in PHY layer, wireless networks can benefit both from the enhancement in channel efficiency and improve the cell-edge performance.

2.5.2. Cooperation in MAC layer

Cooperation techniques in the MAC layer are mostly focussed on forming a cooperation set. Most cooperation strategies involve two phases: the coordination phase and the cooperative transmission phase. Coordination is especially required in cooperative systems since the antennas are distributed among different terminals, but needs to be limited as too much coordination may reduce bandwidth efficiency.

MS cooperation

With this approach, the cooperation happens between MSs. There are two conditions for cooperation: (i) the MS that has good channel conditional (MS1 in the diagram) can provide cooperation and (ii) the data rate of the cooperating MS is lower than the channel capacity. MS cooperation can lead to significant capacity enhancement compared with non-cooperation transmission and can also reduce the transmit power.

Although MS cooperation is theoretically possible, practically it involves many complications because the MSs have to communicate with each other either on a separate frequency or through the BS to exchange cooperative information [40]. This large signalling overhead results in a waste of spectrum and energy which is very important for mobile devices.

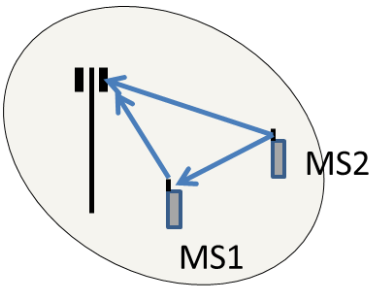

Figure 2.10 Example of MS Cooperation

Relay cooperation

Relaying can be beneficial as well, but it consumes resources from the relaying MSs or relay stations (RS) [41][42]. In relay-based cellular networks, the MSs that cannot establish a direct link, or that have poor channel conditions through a direct link, may transmit through a relay station (RS). However, RS cooperation needs additional spectrum resource to be allocated to the RS in order to provide collaboration [34].

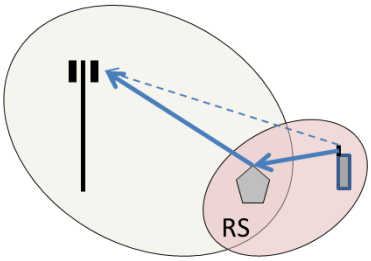

Figure 2.11 Example of RS Cooperation

BS cooperation

BS cooperation assumes that all the BSs, or clusters of BSs, communicate with each other through a central processor that jointly encodes or decodes the MS signals; the also have to transmit the desired signal to the MS simultaneously [41][42][43]. The benefit of BS cooperation is a high capacity gain compared with conventional cellular

systems because the inter-cell interference now becomes the desired signal [35]. This is illustrated in Figure 2.12, where the interfering signal from BS2 is changed to a second instance of the desired signal.

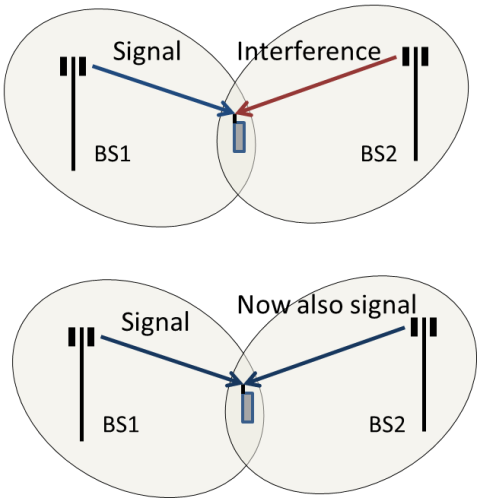

Figure 2.12 Example of BS Cooperation

Since LTE exploits a flat network architecture that connects the base stations, there is an opportunity to coordinate the base antenna transmissions so as to mitigate inter-cell interference, and hence improve spectral efficiency - this allows BS cooperation to be a viable technique for LTE.

2.5.3. Cooperation in PHY layer

In the wireless physical layer, diversity is an excellent means for overcoming fading. However, in some scenarios, the use of multiple antennas might be impractical because of the limited size and coding schemes of the individual nodes. Cooperative transmission has been proposed to address this issue: receivers can receive signals from different paths or channels in order to increase the system robustness and the throughput. However, the performance of cooperative coding scheme is closely related to the interference scenario, so that different cooperation coding schemes are

proposed for different scenarios.

Coded cooperation

Coded cooperation can be viewed as a generalization of decode and forward (DF) relaying schemes where more powerful channel codes (other than the simple repetition codes used in the DF schemes) are utilized in both phases of the cooperative transmission. When using simple repetition codes, the same codeword is transmitted twice (either by the source or by the partner) so decreasing bandwidth efficiency. Instead, in a coded cooperation scheme, different portions of the same message are transmitted in the two phases. Specifically, the source message is encoded in the first portion of the codeword. That is transmitted by the source in Phase I and incremental redundancy (e.g. in the form of extra parity symbols) can be transmitted in the second portion of the codeword by either the source or the partner in Phase II. [44][45]

The coded cooperation assumes that the partner is able to successfully decode the source message in order to re-encode the second portion of the codeword. However, if the partner cannot decode the message, it is unable to generate the second portion of the codeword; instead, it generates and transmits a codeword from its own data. This may introduce additional error.

Superposition coding

Superposition coding has been proposed [46] and shown to be a throughput-optimal encoding technique for unknown interference scenario. Such a scenario can be viewed as a wireless network with inter-cell interference, and therefore the SNR at the receiver, is unknown and time varying. The main idea for superposition coding is to make sure that data can be received successfully even when the interference is severe. Additional information can be received when the interference is small.

Consider K receivers using superposition coding: the transmitter generates K codebooks with certain powers and rates, and transmits the sum of these codewords encoding the symbols intended for the K receivers. The receiver with the worst channel decodes the codeword with the corresponding rate and all the other codewords are indicated as noise. The next-worst receiver is able to decode the rate corresponding to the worst and subtract it from the received signal. Then, it decodes the codewords of its corresponding rate, while it treats all other codewords as noise, and so on.

2.6. Methodology in the thesis

Cooperation in the PHY layer focuses on improving the capacity rate and mitigating the interference impact in an isolated environment. However, such an isolated environment may not be realistic in a network with many simultaneously active terminals. When forwarding information in a cooperative behaviour, cooperative terminal selection and cooperative radio resource allocation should take into consideration.

In general, these schemes are the domain of the MAC layer, and are typically classified into scheduling. Therefore, a cross-layer cooperation scheme combine with PHY layer and MAC layer is necessary.

This thesis considers such an approach.

2.6.1. Introduction of graph theory in network flow

In an LTE network, there are many individual nodes (BS or MS) in the whole network system. However, these nodes may connect each other with different links. One approach is to convert the optimization problem in an LTE network into a graph and find the solution by using graph theory.

Graph theory is a branch of discrete mathematics that attempts to study of the

combination and relationship between objects in mathematical models by the combination of arcs (lines) and vertexes (nodes)[47].

In the communication area, graph theory has been applied to analyze and solve different problems in many areas such as cryptographic protocols and information theory[48] also in wireless communication networks [49][50].

Define a network as a graph[2] with a non-negative capacity $c(e)$ on each edge e and a *source vertex* s and *sink vertex* t. Vertices v are also called nodes. A flow f assigns a value $f(e)$ to each edge e. Write $f^+(e)$ for the total flow on edges leaving v and $f^-(e)$ for the total flow on edges entering v. A flow is feasible if it satisfies the capacity constraints $0 \le f(e) \le c(e)$ for each edge and the conservation constraints $f^+(e) = f^-(e)$ for each node $v \notin \{s,t\}$. Given two locations s, t in the network, the problem is how to find the maximum flow from s to t.

An augmenting path is defined to help finding the maximum flow. When f is a feasible flow in a network N, the augmenting path is a source-to-sink path P in the underlying graph G such that for each $e \in E(P)$,

a) If P follows e in the forward direction, then $f(e) < c(e)$.

b) If P follows e in the backward direction, then $f(e) > 0$.

Let $\varepsilon(e) = c(e) - f(e)$ when e is forward on P, and let $\varepsilon(e) = f(e)$ when e is backward on P. The tolerance of P is $\min_{e \in E(P)} \varepsilon(e)$. When $\varepsilon(e) = 0$, then flow in the graph is maximize. A backward flow on P is not within the scope of discussion.

[2] In graph theory a distinction is sometimes made between "graph" (i.e. main graph) and "assist graph"; for simplicity in this thesis the term "graph" is used throughout.

2.6.2. Introduction to relevant information theory

Information theory addresses two aspects of communication theory:

- what is the ultimate data compression - the entropy H; and
- what is the ultimate communication rate - the channel capacity C [51].

In this thesis Entropy is not considered, but channel capacity is important.

For a communication channel with input X and output Y, define the capacity C by

$$C = \max I(X;Y) \tag{1.1}$$

The capacity is the maximum rate at which information can be sent over the channel and recovered at the output with a vanishingly low probability of error. It should be noted that the *channel capacity* is the *upper bound* on the amount of information that can be reliably transmitted over a communications channel, whereas the *system capacity* means the *maximum achievable transmission rate of a specific communication system employing a certain kind of modulation scheme*. Naturally, the channel capacity ≥ system capacity and the nearer the system capacity is to the channel capacity the better.

In a MIMO scenario, a single capacity measure may not be the best means of assessing the performance of each user. An extension is to establish a region for each user in order to evaluate the performance and this is considered below.

Sum-rate performance

In a wireless networks, a transmitter will have many different messages and each one needs to be sent to a different receiver. The *sum-rate capacity* of a system is defined as the capacity of transmitting all the messages at the same time and is widely used in order to evaluate the system performance theoretically

[52][53][54][55] .

In the cellular context, both uplink and downlink communication channels can be classified as Gaussian interference channels. The concept of BS cooperation in a cellular system can convert the uplink and the downlink interference channels into a MIMO Multiple Access Channel (MAC) and a MIMO Broadcast Channel (BC), respectively. The capacity regions of these MIMO channels have been found [56] and they can be interpreted accordingly in the context of cooperative cellular systems. It is shown in [57] that a MIMO multiple access channel can be obtained from a general uplink interference channel, introducing cooperation among BSs. Similarly, [58] shows that a MIMO broadcast channel can be formed from a general downlink interference channel by allowing BS cooperation. The main objective of this BS cooperation is to convert the unwanted interference power into useful signal power. An example is given in Figure 2.13.

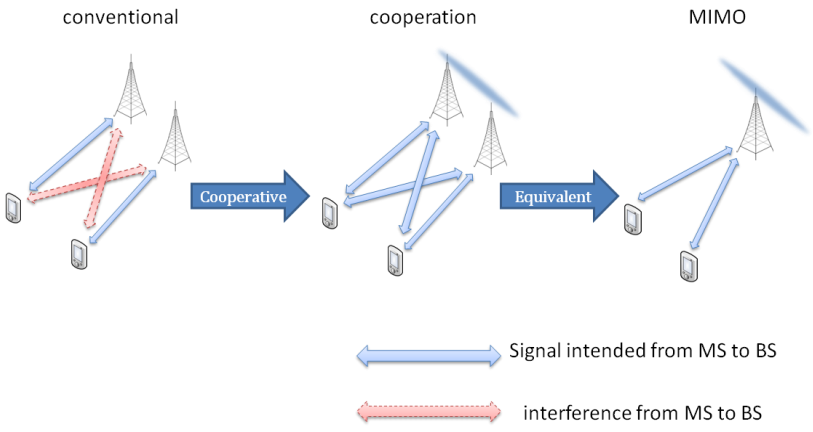

Figure 2.13 Example of BS cooperation

2.7. Summary

This chapter has introduced the concepts in LTE network that are relevant to this thesis, including the basic concept of MIMO, the basic concept of cooperation and the relevant research of cooperation in cellular networks. Also, the concept of sum-rate capacity has been.

3. Simulator for cooperation LTE Networks

Using a cooperation approach in the MAC layer is important, as this can assist the system to choose the proper cooperation users. To research this, a system-level simulator has been built by the author.

This simulation platform was built based on an existing downlink OFDMA system level platform[3]; all the modules have been modified to produce a downlink cooperative LTE-A system level platform and the algorithms proposed in this thesis were added in to this platform. All of this work has been done by the author. The simulator is designed based on IEEE 802.16j, and Long Term Evolution (LTE). The details of the modules are given in section 3.3.

3.1. Overall Design of Simulation Platform

The simulator uses time-stepping (rather than being event driven) with each time step being one TTI. Figure 3.1 indicates the flow chart of simulator.

For each drop, the initialization module runs in order to create the network topology, including initializing the position of BSs and MSs, computing large scale pathloss and shadow fading, choosing the anchor BS for each MS, and calculating the potential cooperative BSs' set.

After the initialization, the simulator operates following a TTI-based function.

- The CQI feedback module collects CQI information for the user on its scheduled RB and feeds back the CQI to BS. The CQI information includes not only the non-cooperative MS, but also the cooperative MS.

- After collecting the CQI information, the cooperative set would be generated

[3] The existing simulation platform was produced by the author and his colleagues as part of a Masters degree in BUPT according to [62]-[72]. The simulation platform is verified and validated by the China Academy of Telecommunication Research of MIIT

according to the appropriate scheme.

- A scheduling module will allocate a RB to each MS. For the non-cooperative MS, the RB will be selected in its anchor cell. For cooperative MSs, the RBs will be selected jointly from its cooperative set.

- The interference calculation module operates to obtain and upgrade the precoding and equalization matrix. It calculates the SINR for use on the scheduled RB and stores this information in the CQI module.

- The system performance statistics module activates last in order to calculate the statistics of system performance, including data rate and which RBs are scheduled.

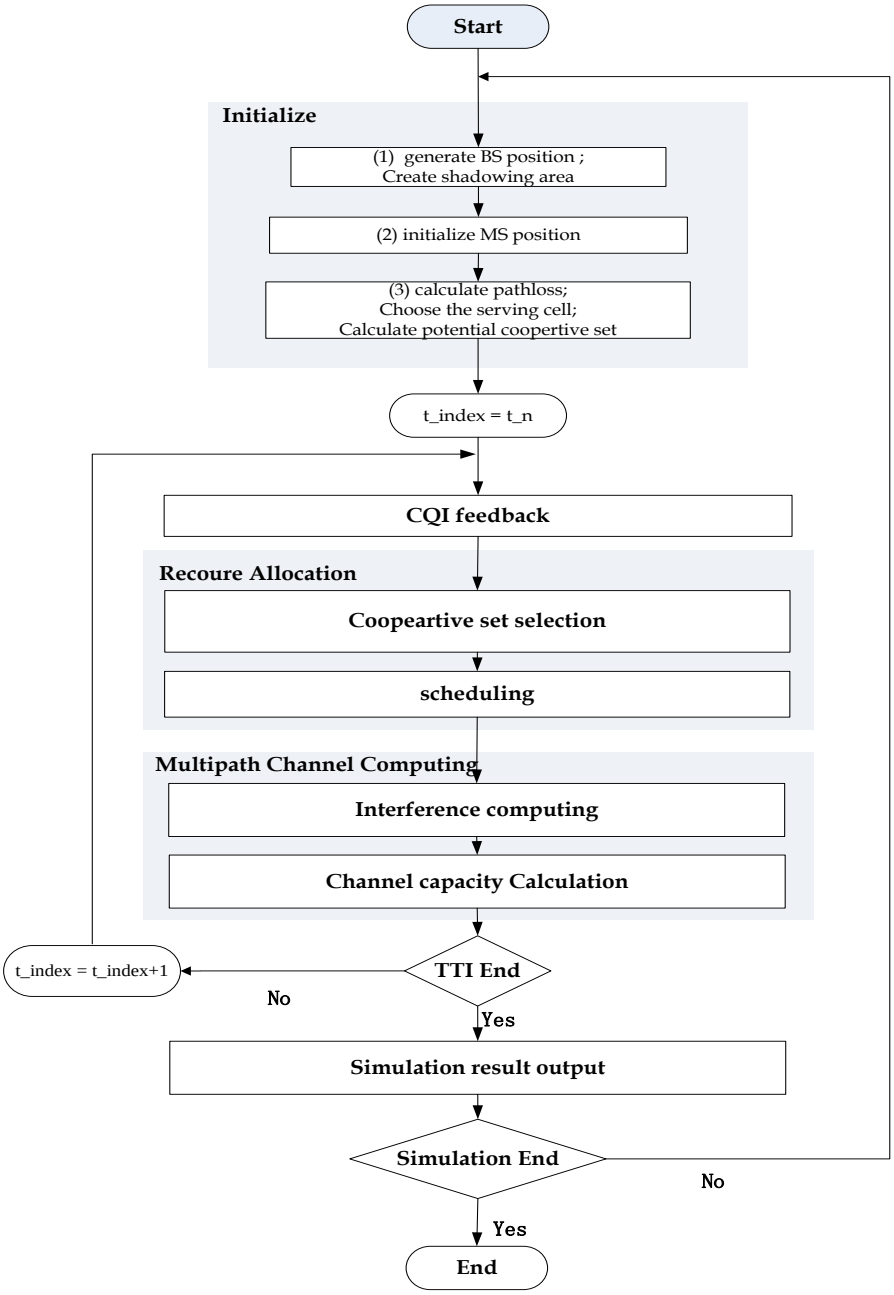

Figure 3.1 flow chart of simulator

3.2. Parameters in Simulator

A downlink cooperative LTE-A system is considered here. In the LTE system, every 12 continuous subcarriers compose a physical resource block (PRB), which is used for resource allocation in the frequency domain. One transmission timing interval (TTI) is 1 ms, and each TTI is used for resource allocation in time domain. Parameters of

the downlink simulator are listed in Table 3.1.

Table 3.1 Downlink transmission parameters

Parameter	Value
Transmission Bandwidth	10 MHz
TTI	1 ms
Subcarrier spacing	15kHz
Number of subcarriers occupied	601 [-300,300]
Number of subcarriers in use	600, subcarrier # 0 is not used
PRB	50
Subcarriers/PRB	12 (consecutive)
PRB BW (kHz)	180

An urban macro-cell scenario is considered in the simulation platform; the details of the parameters are defined in [59] and are listed in Table 3.2.

The channel model used is from 3GPP TR 25.996; this is described in section 3.4.

Table 3.2 System level simulation parameter of Macro-cell

Parameter	Value
Cellular Layout	Hexagonal grid, 7 cell sites
Number of Sectors per Cell	3
Inter-site distance	500 m
Antenna Configuration	1×2
Central Frequency/Bandwidth	2.0 GHz/10MHz
BS transmit power	46dBm
Minimum distance between MS and BS	>= 35 meters
Thermal noise density	-174 dBm/Hz
Penetration Losses	20 dB

BS Antenna pattern(horizontal) (For 3-sector cell sites with fixed antenna patterns)	$A(\theta) = -\min[12(\frac{\theta}{\theta_{3dB}}), A_m]$ $\theta_{3dB} = 70°, \quad \mathrm{A_m} = 20dB$
Number of simulation drops	10
Simulation time per drop	500TTI

A wrap-around model is used in the simulator as in 3GPP CR1002. Each cell contains three sectors structure (as in 3GPP TR36.942) and, to maintain high frequency efficiency, the frequency reuse factor equals to one, i.e., all three sectors use the same spectrum. To mitigate the intra-cell interference between sectors, a directional antenna is deployed in each sector.

In regular operations, each MS is registered at and communicates with a single BS, which is called the anchor (or serving) BS. However, in the cooperative scenario the MS will communicate simultaneously with more than one BS. The set of potential cooperative BSs (also known as the diversity set - defined in the IEEE 802.16e standard) keeps track of the anchor BS and neighbouring BSs that are within the communication rage of an MS. Note that the elements within the diversity set depend on the threshold definition method.

3.3. Module Functions and Implementation

The functions of the main modules of the simulation platform are briefly described in this section.

3.3.1. Initialization Module

Function description:

- creates network topology, including (i) initializing the position of BS and MS, (ii) computing large-scale pathloss and shadow fading, (iii) choosing the anchor BS for each MS, and (iv) calculating the potential set of

cooperative BSs;

- initializes all the parameters of the system.

Existing work:

Initialize the position of BS and MS, with MSs being distributed uniformly. According to the distance between BS and MS, the large-scale pathloss and shadowing are computed. The serving cell for each MS is decided by the maximum SNR value.

Extension work:

Different MSs distribution methods can be selected: for example, hot spot distribution, uniform distribution, different percentage of cell-edge users distribution. Due to the requirement of cooperation, the initialization module not only selects the anchor cell but also selects a potential cooperative set (also known as diversity set) available to each user by setting up a SNR threshold.

Input: none

Output: pathloss, shadow fading, potential cooperative set, all related parameters of the system

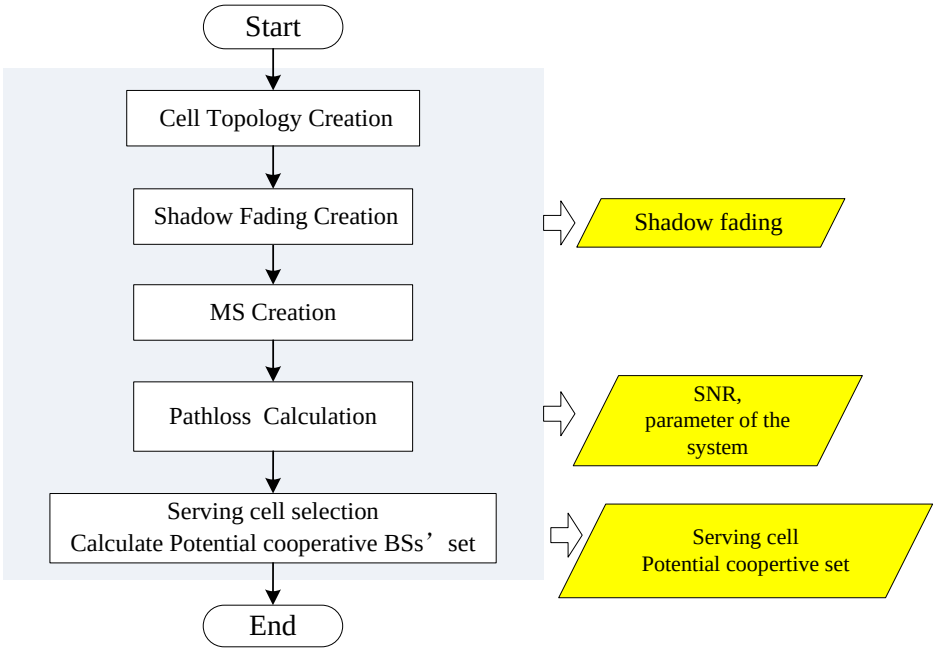

Figure 3.2 Flow chart of initialization module

In this module, a 19 hexagonal cellular topology structure is constructed with each cell composed of 3 sectors. Then a shadow fading map is created based on the 19 cells. MS creation is iterative, sector by sector, and the anchor cell selection is based on the result of the pathloss calculation.

3.3.2. CQI Feedback Module

Function description:

- (i) creates multipath fading channel, (ii) upgrades the CQI information for the user on its scheduled RB; and (iii) feeds back the CQI to the BS;
- SINR of users on all PRBs is collected in this function, which will be stored for several TTIs, then it outputs the CQI to other modules as feedback delay behaviour.

Input: SINR in current TTI

Output: SINR in previous TTI as a feedback delay behaviour

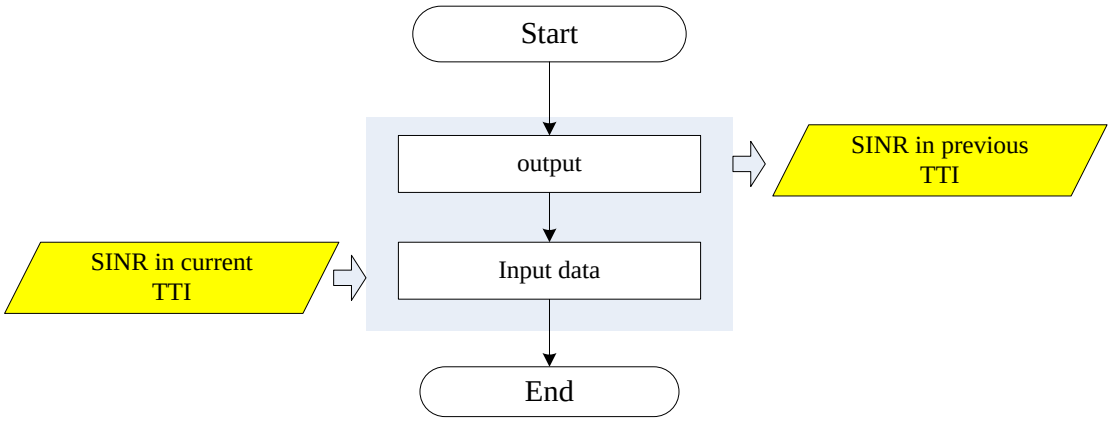

Figure 3.3 Flow chart of CQI feedback module

Here it is assumed that the feedback delay is 10ms (10 TTI). Therefore, a 10 element vector is defined in this function in order to store the SINR value. This function can collect the SINR per TTI, and send SINR following the first-in first-out rule.

3.3.3. Resource Allocation Module

Function description: Based on the CQI from the CQI feedback module, resource is allocated to users according to the resource allocation algorithm. The resource includes two sub-functions: (i) cooperative BS selection and (ii) PRB allocation.

Existing work:

Round robin & maximum C/I as two candidate scheduling methods; scheduling module operates and selects the proper RB for MS in each BS individually.

Extension work:

Proportional fairness scheduling method is introduced in this module. The individual scheduling method is not suited for the requirement of cooperation.

Therefore, joint scheduling is applied. For non-cooperative MSs, the scheduling module searches the proper RB in its anchor BS only. For cooperative MS, the scheduling module searches the proper RB in its cooperative set by jointly considering the available RB in each BSs and the performance.

Input: potential cooperative set, SINR

Output: cooperative set, PRB for users

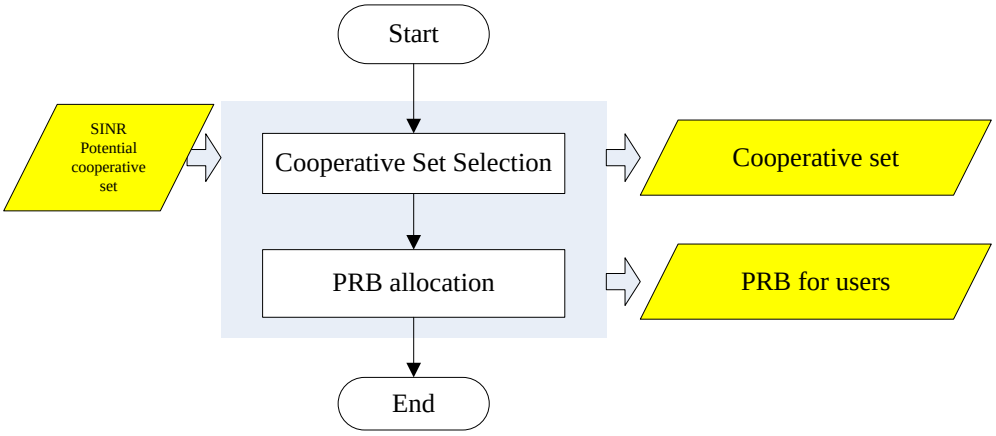

Figure 3.4 Flow chart of resource scheduling module

The sub-function of cooperative set selection contains two procedures: (i) upgrade the potential diversity set and (ii) select the cooperative set from the diversity set according to the defined algorithm.

In the traditional LTE system, each cell schedules its own PRB individually. However, in a cooperation scenario, PRB allocation requires a coordinated behaviour. Therefore, the traditional scheduling scheme (for example, round robin, max C/I, or proportional fairness) cannot achieve the requirement of the cooperation network [60]. Hence, two coordinated scheduling scheme are deployed in the simulator in order to investigate the system performance.

In the SU-MIMO scenario, a fixed cooperation frequency scheme is deployed [61]. By

treating cell-centre users and cell-edge users differently, a cooperation frequency zone is introduced as a possible candidate to perform cooperation SU-MIMO operation within the cluster for the cell-edge users. The division of the system bandwidth can be illustrated in Figure 3.5.

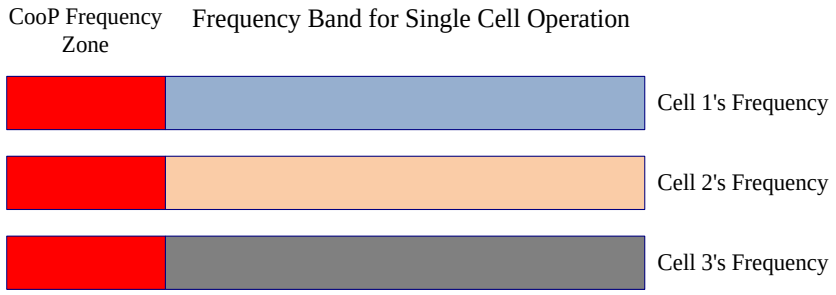

Figure 3.5 Frequency allocation of SU-MIMO

In the single cell operation frequency zone, each cell schedules individually for non-cooperative users. In the cooperative frequency zone, the cells in the same cluster jointly schedule the PRB for cooperation users. To trade-off the performance and fairness, the proportional fairness algorithm is deployed.

3.3.4. Interference Computing Module

Function description: the SINR for users on scheduled PRBs is calculated in this function by using BS transmit power, the large scale fading seen by the users, multi-path fading, co-channel interference from other cells, and AWGN. It also records users' capacity per TTI by using Shannon's formula.

Existing work:

Interference computing module calculates the SINR by using Shannon's equation. The typical singular value decomposition (SVD) method is used for each MS to generate the precoding matrix.

Extension work:

For the cooperative scenario, an adaptive SINR calculation method is proposed. For non cooperative MSs, the traditional method is still used in order to obtain the SINR. For the cooperative MSs, the desired signal strength is computed from the cooperative set instead of the anchor cell only. The traditional SVD precoding method is not suited to the cooperative scenario.

Therefore, for non cooperative users, still using SVD decomposition of the matrix, the precoding matrix is determined and sent to the BS. For cooperative users, multiple BSs will transmit signals generated by the precoding matrix jointly according to the method in [62].

Input: cooperative set, PRB for users, large scale fading, transmit power

Output: SINR, users' capacity

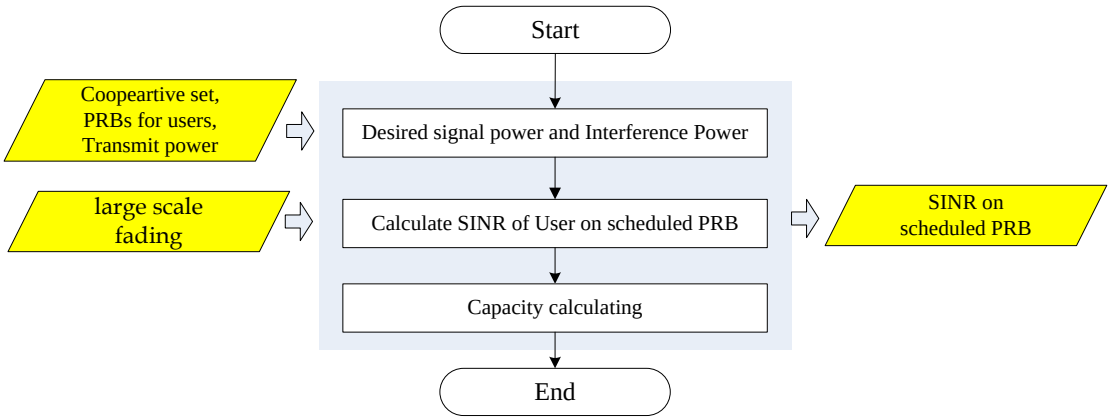

Figure 3.6 Flow chart of multipath channel computing module

A precoding technique is used in the LTE downlink. The MS can obtain the impulse response between the transmit antenna and receive antenna by channel estimation in the frequency domain. These impulse responses compose a matrix. For non cooperative users, using SVD decomposition of the matrix, the precoding matrix is determined and sent to the BS. For cooperative users, multiple BSs will transmit

signals generated by the precoding matrix jointly according to the method in [62].

3.4. Channel Module

3.4.1. Pathloss Model

The following are assumptions made for the urban macro-cell environment:

- BS antennas are above rooftop height
- The macro-cell pathloss is based on the modified COST231 Hata urban propagation model [63]:

$$\begin{aligned} PL &= (44.9 - 6.55\log_{10}(h_{bs}))\log_{10}(\frac{d}{1000}) + 45.5 \\ &+(35.46 - 1.1h_{ms})\log_{10}(f_c) - 13.82\log_{10}(h_{bs}) + 0.7h_{ms} + C \end{aligned} \quad (3.2)$$

Where *PL* detions the pathloss, h_{bs} is the BS antenna height in metre, h_{ms} the MS antenna height in metre, f_c the carrier frequency in MHz, d is the distance between the BS and MS in metre, and C is a constant factor ($C = 3dB$ for urban macro). Setting these parameters to [64] $h_{bs} = 32m$, $h_{ms} = 1.5m$, and $f_c = 1900MHz$, the pathloss for urban macro environments become, $PL = 34.5 + 35\log_{10}(d)$. The distance d is required to be at least 35m.

3.4.2. Shadow Fading Model

A normal-distributed random variable is usually used in simulation; this refers to typical log-normal shadow fading model. To simplify the module, the non correlation of shadow fading is taken into account; the standard deviation value is 8dB under NLOS transmission [65].

3.4.3. Multi-path Fading Model

The spatial channel model extension, SCME, is described in [66], and it widens the applicability of SCM. The limitation of SCM mainly comes from the fact that the maximum number of multi-paths in the SCM model is limited to six. SCME extends this by incorporating an intra-path delay spread. When the intra-path delay is zero, the SCME model collapses to the SCM model. The approach of intra-path delay spread was originally proposed for indoor propagation modelling in [68]. A similar model was specified for outdoor propagation modelling in [69].

Table 3.3 Intra-cluster parameters for SCME

Mid-path	Number of sinusoids and power	Delay	Sub-paths	AS_i / AS_n
1	10 (of 20)	0	1,2,3,4,5,6,7,8,19,20	0.9865
2	6 (of 20)	25 ns	9,10,11,12,17,18	1.0056
3	4 (of 20)	50 ns	13,14,15,16	1.0247

Consider an example of the SCME implementation that was proposed for LTE performance evaluation with 10 MHz bandwidth [63]. In this model, the nth $(n = 1, 2, \ldots, N)$ multi-path is further decomposed into three mid-paths $(i = 1, 2, 3)$ providing a maximum of 18 mid-paths $(N = 6)$ as shown in Table 3.3. Each mid-path then consists of a number of subpaths corresponding to that multi-path. The number of subpaths for the first, second and third mid-paths within the nth multi-path is 10, 6 and 4 respectively as shown in Table 3.3.

Since the power for all the subpaths within a multi-path is the same, the power for the ith mid-path $(i = 1, 2, 3)$ within the nth path $P_{n,i}$ is given as:

$$P_{n,1} = \frac{P_n}{2},\ P_{n,2} = \frac{3P_n}{10},\ P_{n,3} = \frac{P_n}{5} \tag{3.3}$$

This means that the first, second and the third mid-path contains 50%, 30% and 20%

of the multi-path respectively. The relative delay offset for the first, second and third mid-paths within the $nth\,(n=1,2,\ldots,N)$ multi-path are 0, 25 and 50 ns respectively. This assumes a delay resolution of 1/4 of the sampling rate for 10MHz bandwidth $(\frac{1}{4\times 10MHz}=25ns)$.

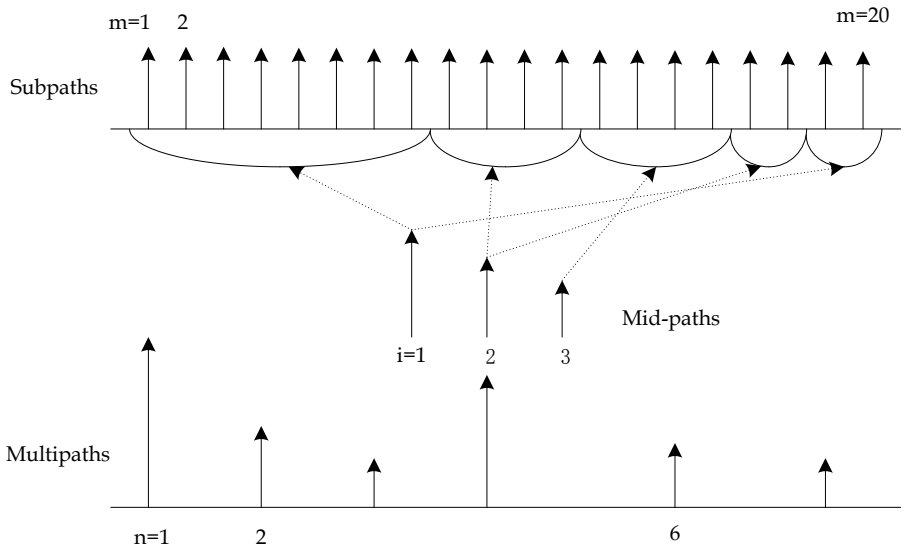

Figure 3.7 Relationship between time- and frequency-domains in SCME model

In the SCM model, each subpath $(m=1,2,\ldots,M,\quad M=20)$ has a fixed angle relative to the path mean angle assigned to it. By perturbing the set of subpaths assigned to a mid-path, the angular spread (AS) of that mid-path can be varied. The mid-path angle spreads AS_i were optimized such that the deviation from the path angle spread AS_n that is the angle spread of all mid-paths combined is minimized.

The details of tap delay are given in Table 3.4.

Table 3.4 Tap delay line for SCME

Scenario		Suburban Macro		Urban Macro	
Power-delay parameters: relative	1	0.0	0.00	0.0	0.00
	2	137.5	-2.67	362.5	-2.22

delay (ns)/ path power (dB)	3	62.5	-6.21	250.0		-1.72	
	4	400.0	-10.41	1037.5		-5.19	
	5	1387.5	-16.47	2725.0		-9.05	
	6	2825.0	-22.19	4600.0		-12.50	
Resulting total DS (ns)		231.0		841.1			
Path AS at BS, MS (deg)		2, 35		2, 35			
Angular parameters: Angle-of-Arrival (deg) / Angle-of-Departure (deg)	1	156.2	-101.3	65.7	82.0	76.5	-127.3
	2	-137.2	-100.9	45.6	80.5	-11.9	-130.0
	3	39.3	-111.0	143.2	79.6	-14.6	-136.8
	4	115.2	-113.0	32.5	98.6	17.7	-96.2
	5	91.2	-115.5	-91.1	102.1	167.7	-159.6
	6	4.7	-118.1	-19.2	107.1	139.1	173.2
Resulting total AS at BS, MS (deg)		4.7, 64.8		7.9, 62.4		15.8, 62.2	

3.5. Verification and Validation

The simulation platform is an important part of the work of this thesis. The simulation was built using C++ and Matlab and has been debugged line by line. In addition, results were obtained for specific scenarios to show that the simulator is working correctly.

3.5.1. Verification

The channel module is verified by the large-scale and fast fading. A result for G-factor [4] distribution is given in Figure 3.8, which shows the cumulative distribution function (CDF) curve of G-factor value (in dB). The G-factor value ranges from -5 dB to 16 dB, and it is 2dB when the probability value is 0.5. This result complies with the evaluation results in [70][71] and so verifies the pathloss fading

[4] The G-factor is a parameter only considering the large scale fading impact. It is using to evaluate the received signal strength compare the interference and noise. The G-factor is $G = \frac{P_S}{\sum_{i \in M} P_{I,i} + N}$

design.

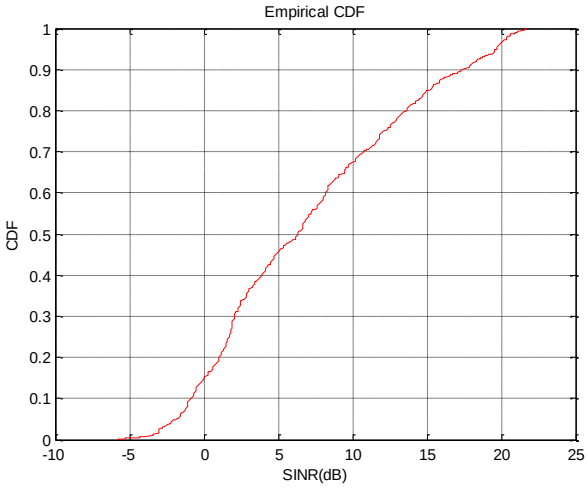

Figure 3.8 G-factor distribution

The multipath fading channel CDF curve is shown in Figure 3.9. Each tap of the envelope of the multipath fading is Rayleigh-distributed with mean $\sqrt{\frac{\pi}{2}}\sigma$ and variance $\frac{4-\pi}{2}\sigma^2$. According to [72], since normalized transmission power is used in multipath fading, the value of $\sigma = 0.7071$. The results in Figure 3.9 show a mean 0.9563 and variance 0.3185, which complies with the result in [72].

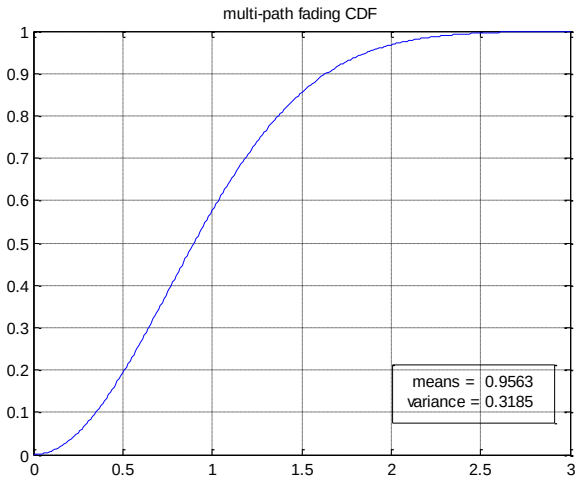

Figure 3.9 CDF of fast fading

3.5.2. Validation

The simulator is validated for two parts: i) user distribution ii) cooperative threshold definition.

User distribution

Two distribution methods are used here: uniform distribution and hot-spot distribution (the hot spot MSs are generated first and the remaining ones have uniform distribution). In each cell, the distribution of the MSs is different, which satisfies the user random distribution characteristic.

To validate that this part of the simulator is working properly, the distribution of users for the two different scenarios was plotted and checked by hand to make sure the distributions were as expected.

Cooperative threshold definition

In the previous subsection, the simulator has been validated. In this subsection, the simulator is run in order to find a proper cooperative user threshold, which is one of the important parameters in a cooperation system [72][73]. The G-factor (discussed earlier) is used to assist in deciding the cooperation threshold. However, by utilizing cooperation behaviour, the propagation power from the cooperative cell becomes part of the desired signal instead of interference, and then the G-factor becomes:

$$G' = \frac{P_s + \sum_{i \in C} P_{I,i}}{\sum_{i \in M, i \notin C} P_{I,i} + N} \tag{3.4}$$

Where C denotes the cooperative set, M denotes the set of cell, P_s denotes the transmit power from serving cell and N denotes the thermal noise. From (3.4), the gain of the G-factor is proportional to the size of C, which means that the more cooperative cells there are, the better the SINR that will be received for the

cooperative user, but at the same time it will take more RBs during the transmission. To trade-off frequency efficiency and the QoS, the size of the cooperative set in this simulation is smaller than or equal to 3 [64].

To decide whether to have cooperative or non-cooperative behaviour, a proper threshold value is needed. Table 3.5 shows the percentage of cell-edge users for different thresholds in the simulation. Generally, the percentage of cell-edge users should be under 20% in order to achieve reasonable performance.

Table 3.5 Percentage of cell-edge user in different threshold

Threshold(dB)	-3	0	3
Percentage of cell-edge users	4%	16%	33%

According to the CDF function shown in Figure 3.10, there are three different values -3dB, 0dB and 3dB around the 20% point. Therefore, the three different values (-3dB, 0dB and 3dB, respectively) are chosen as candidates in this subsection in order to defined a proper cooperative threshold.

By utilizing the three different thresholds, the CDF functions for the G-factor are shown in Figure 3.10.

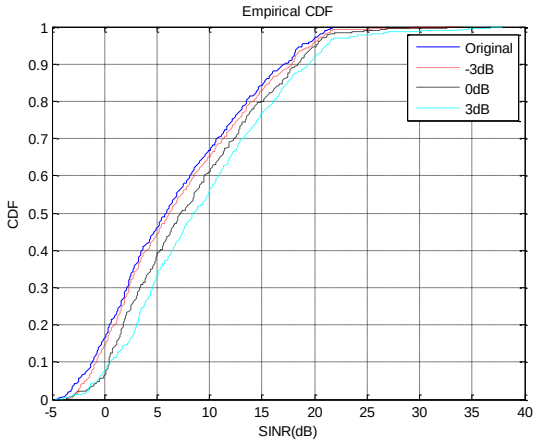

Figure 3.10 G-factor in different threshold

Figure 3.10 indicates the CDF curves move to the right as the threshold value becomes larger and larger, which means the SINR for the cooperative users becomes better and better. However, as the threshold value becomes larger, more users are allocated as cooperative users. This increases the signalling exchange during the cooperation operation. Moreover, too many cooperative users aggravate the lack of RBs in the conventional network.

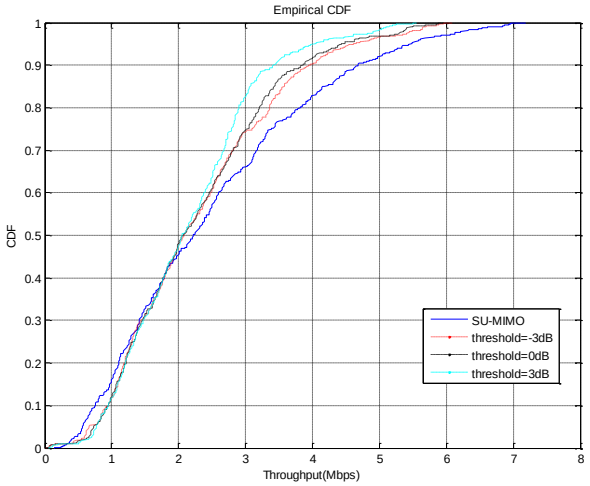

Figure 3.11 throughput CDF in different threshold

Figure 3.11 indicates the system throughput CDF for different thresholds. By utilizing the cooperation scheme, the left part of the curves moves to the right compared with SU-MIMO. It means the performance of the low throughput users improved. However, the right part of the curves moves to the left compared with SU-MIMO, meaning the performance of high throughput users decreases. The detail of the cell-edge spectrum efficiency and cell average spectrum efficiency are shown in Table 3.6. It reveals the cell-edge spectrum efficiency increases when the threshold increases. However, when the threshold increases from 0dB to 3dB, the cell-edge spectrum efficiency increases only a little compared with the reduction in cell average spectrum efficiency. That is because too many users are allocated as cooperative users so aggravating the lack of RBs. Therefore, 0dB is defined as the

cooperative threshold in the thesis.

Table 3.6 detail of spectrum efficiency

	Threshold (dB)	cell-edge spectrum efficiency (bps/Hz)	cell average spectrum efficiency (bps/Hz)
Non cooperative	-	0.0569	2.4469
Cooperative	-3	0.0663	2.2994
	0	0.0737	2.2671
	3	0.0775	2.1561

3.6. Summary

A description of the overall design of the simulation platform and system parameters has been given in the first part of this chapter, together with the system parameters. This is followed by a more detailed explanation of the most important modules. The channel model is introduced in the end of this chapter including pathloss model, shadow fading model and multi-path fading model. Validation of the simulator shows it is operating correctly. A 0dB cooperative threshold is set in order to obtain the results for the rest of the thesis based in the results in 0.

4. Intra-cell graph-based transmit antenna selection

4.1. Introduction

Distributed MIMO (D-MIMO) systems employ multiple antennas at both BS and MS [57][78], so the total number of antennas in a D-MIMO system is greater than in a conventional centralized antenna system (CAS). Therefore, intra-cell transmit antenna selection is a key problem for the practical application of D-MIMO systems. To tackle the decision-making problem, a Graph-based transmit antenna selection (GBTS) algorithm is proposed to find the most suitable transmit antennas dynamically according to the different channel state information. The aim of this algorithm is to maximise the system throughput.

It is well-known that in a multi-cell OFDMA scenario, inter-cell interference limits the performance of cell-edge users [79]. Cooperation techniques in the MAC layer can be used to improve the system performance of users at cell edge [80]-[85]. Therefore, multi-cell transmit-antenna-selection considering inter-cell interference has been studied. Based on a multi-cell cooperation model, a graph-based transmit antenna selection algorithm has been implemented in the research described in this thesis. Different utility functions have been designed for different optimization objectives (system throughput and user fairness) and a modified *max-flow min-cut* graph theory established and proved mathematically as a solution of transmit antenna selection. The performance of this algorithm has been investigated by simulation.

4.2. System Model

The cooperation distributed system considered in this Chapter [79], sometimes referred to as network MIMO [82], uses a main-remote type base station architecture. This type of architecture splits the baseband functionality and RF into two parts: Base Band Unit (BBU) and Radio Remote Unite (RRU) [83], as shown in Figure 4.1

Example of cooperation system, are deployed in each cellular. All the RRUs are connected to and controlled by the BBU through a wired link. Therefore, the sector antennas may be placed in geographically disparate locations. In this way, a collection of conventional cells would be grouped together in order to form a larger cooperative cell. It is assumed that the channel condition between the BBU and its RRU can be regarded as perfect without fading and delay.

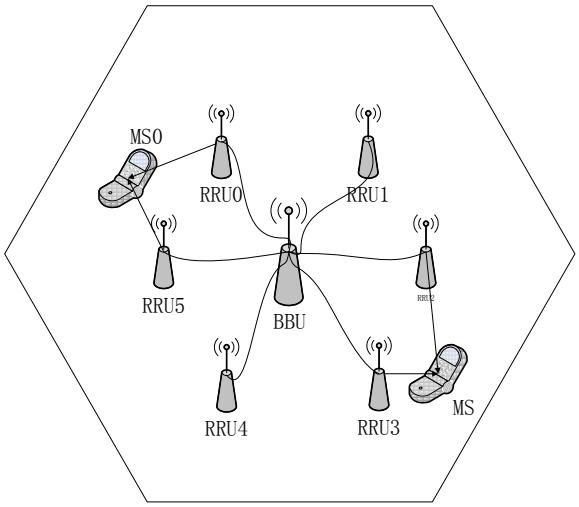

Figure 4.1 Example of cooperation system

Each BBU has a set of RRUs distributed around the BBU (in the literature often at a radius of half the cell radius), each RRU having one transmit antenna. The MSs, each with multiple receive antennas, are distributed across the cells BBUs.

In a cooperation scenario, each MS is registered at one BBU but communicates with a set of BBUs, called the cooperative set. The SINR expression with cooperation has to take into account the set of interfering. i.e., the downlink transmit power from RRUs will cause interference to an MS.

By utilizing the SNR between RRU and MS, the BBUs can evaluate the channel condition for each MS.

Trying to determine the maximum system throughput this leads to a combinatorial

NP-hard problem. In order to obtain an optimal solution, a graph theory approach is used to solve the problem. In optimization theory, the maximum flow problem is to find the maximum feasible flow through a single-source, single-sink flow network.

4.3. Transmit Antenna Selection algorithm

4.3.1. Problem Formulation

A graph is generated in this section. The Ford-Fulkerson algorithm [87] can be used to achieve the maximum flow. One of the characteristics of the Ford-Fulkerson algorithm is the result does not depend on the order of choosing the edge. Therefore, a modified Ford-Fulkerson algorithm is proposed with a single-source single-sink directed graph in order to achieve the maximum network flow and the maximum edge weight.

Use the notation $\mathcal{G}(\mathcal{V}, \mathcal{E})$ to represent a graph where $\mathcal{V}$ and $\mathcal{E}$ denote the sets of vertices and edges respectively. In this chapter use the formulation of the graph as $\mathcal{G}(\mathrm{N}, \mathrm{M}, \mathcal{E})$ where $\mathcal{V}(\mathrm{N})$ and $\mathcal{V}(\mathrm{M})$ denote the set of RRUs and MSs, respectively. Each edge (from set $\mathcal{E}$) contains a capacity. The capacity of $\mathcal{E}(\mathrm{S}, \mathrm{N})$ is used to represent the available RBs; the capacity of $\mathcal{E}(\mathrm{N}, \mathrm{M})$ is used to represent whether the RRU is assigned to the MS. Furthermore, $\mathcal{E}(\mathrm{N}, \mathrm{M})$ contains weights that represent the SNR between the RRU and MSs. The capacity of $\mathcal{E}(\mathrm{M}, \mathrm{D})$ is used to represent the number of the transmit antenna with upper bound $\mathrm{N_T}$.

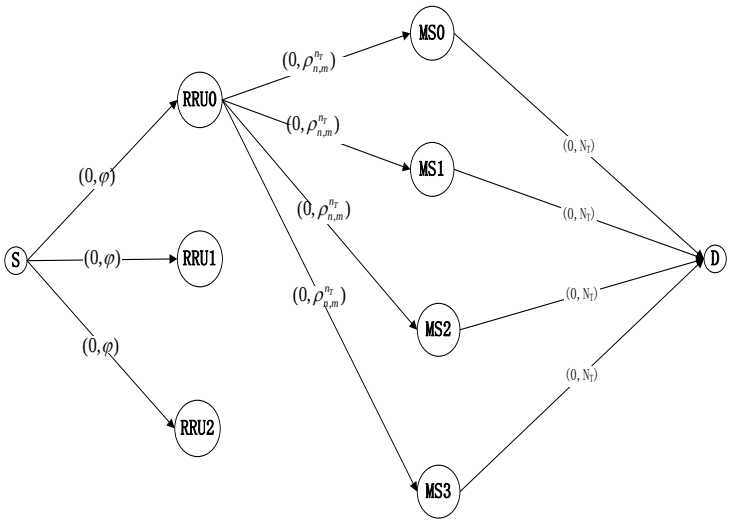

Figure 4.2 Transmit power and data rate based directed graph

4.3.2. Procedure of Transmit Antenna Selection algorithm

A graph based transmit antenna selection algorithm (GBTS) is proposed in this section. The Ford-Fulkerson algorithm [47] is one method to achieve the maximum flow. As mentioned above, one of the characteristics of the Ford-Fulkerson algorithm is the result of maximizing the flow does not depend on the order of choosing the edge [49], so a heuristic algorithm is proposed building on this characteristic. For a single-source and single-sink directed graph, the heuristic algorithm will start at the source node. GBRS searches the edge with largest weight between source node and RRU nodes. If the edge can be augmented, then choose the edge and move to the RRU node and search MS node until it finds an augmenting edge. Otherwise, the source node will keep on searching its adjacent RRU nodes according to the weight of the edge until it finds the augmenting edge. When the augmenting path reaches the sink node, calculate the minimum residual between flow and capacity for all edges on the path. Increase each flow with residual on $\mathcal{E}(\mathrm{S},\mathrm{N})$, $\mathcal{E}(\mathrm{N},\mathrm{M})$ and $\mathcal{E}(\mathrm{M},\mathrm{D})$, which means a resource clock RB is occupied, assign the RRU to the MS and generate the $\mathrm{N_T}$ transmit antenna array. This procedure will be carried on until this is no

augmenting path between source node and sink node. The procedure of the heuristic algorithm is described as follows:

Step 1: For each path from source to sink, choose the path with maximum weight in each edge.

Step 2: If the path is not an augmenting path, the procedure is carried on until an augmenting path is found.

Step 3: Let residual = minimum of (flow - capacity) for all edges on the path.

Step 4: Increase the flow of each residual on the path.

There are two constrains in the algorithm. Due to the constraints of the edge $\mathcal{E}(N, M)$, each RRU will only be allocated MSs with the number of available RBs. The constraints of the edge $\mathcal{E}(M, D)$ will promise there are N_T RRU to generate the transmit antenna array.

The proposed Ford Fulkerson algorithm not only has the maximum network flow, but also has the maximum sum weight of edges.

4.3.3. Definition for User Fairness

Fairness is an important consideration in most performance studies. Particularly in distributed systems, where a set of resources is to be shared by a number of users, fair allocation is important. In communication networks, some want equal delay, others want equal power for all users sharing a resource. Use a weighting factor m [96][47] for the MSs nodes that is given by Jain index; this is evaluated on a time-windowed basis:

$$m(n+1) = \frac{R_m(n)}{T_m(n)} \tag{4.1}$$

Where $m(n+1)$ is the weighting factor for window $n+1$, $R_m(n)$ is the data rate for the mth user and $T_m(n)$ is the average throughput for the mth user, both in the past window; m is updated according to [89]

$$T_m(n+1) = \begin{cases} (1-\frac{1}{t_c})T_m(n) + (\frac{1}{t_c})R_m(n), & m = m^*(n) \\ (1-\frac{1}{t_c})T_m(n) & m \neq m^*(n) \end{cases} \quad (4.2)$$

Where t_c is the window length that can be adjusted to maintain fairness over a determined time horizon and $m^*(n)$ denotes the chosen MS. If there is positive change for MS m, it will decrease the priority of MS m in the next window slot. This mechanism permits user fairness

The whole point about the transmit antenna selection algorithm is that it can increase the cell-edge users throughput. However, this operation will lead to a reduction in the data rate fairness among users because the GBTS algorithm will always satisfy the MS requirement according to the sort by the MSs as explained before. The MS at the top is always has the highest priority so that a function to improve the user fairness has to be defined.

4.3.4. Solution of GBTS-F

It is hard to provide service simultaneously in a slot when the number of cooperative users is larger than the radio resource; unfair service will be provided, since the primary goal of scheduling is to maximize capacity. The basic heuristic algorithm described previously can achieve the maximum rate, but with no promises on the fairness. Therefore, a proportional fairness mechanism is considered. In this chapter, the fairness is evaluated in terms of throughput. The fairness index is given according to [50]

$$F = \frac{(\sum_{m=1}^{M} r_m)^2}{M \sum_{m=1}^{M} r_m} \tag{4.3}$$

Where r_m denotes the throughput of MS m. The fairness index F is a value between 0 and 1, in which $F=1$ means 'fair'. By introducing the fairness mechanism, the procedure of the proposed heuristic algorithm becomes:

Step 1: Initialize all edge's cost to 0;

Step 2: Sort the MS according to (4.2) by descending order;

Step 3: Choose MS according to the sort set. Find the transmit antenna according to

$$\mathrm{n_T} = \arg\max_{\mathrm{n_t} \in \mathrm{N_T}} \mathcal{E}(\mathrm{n_T}, \mathrm{M})$$

Step 4: If the path is not an augmenting path, the procedure is carried on until an augmenting path is found.

Step 5: Let residual = minimum of (flow - capacity) for all edges on the path.

Step 6: Increase the flow of each residual on the path.

Step 7: If there is an augmenting path in the graph, go to step 4, otherwise go to 9.

Step 8: the edge $\mathcal{E}(\mathrm{N_T}, \mathrm{M}) = 1$ denote to the antenna $\mathrm{N_T}$ is assigned to MS M

The complexity of this method iso$(\mathrm{n}^3 + \mathrm{nlogn} + \mathrm{n})$.

4.4. Performance Simulation and Analysis

In this section, the performance of the proposed scheme is studied by simulation. Three schemes are tested: (i) a non-cooperative scheme, (ii) a static cooperative scheme [91] and (iii) GBTS. A proportional fairness (PF) scheduling with additional BSs overhead exchange is used for RB allocation. The system throughput is the sum

of the average throughput achieved in all cells.

Figure 4.3 is the system throughput with different numbers of MSs. The system throughput increases as the user number increases, but the simulation result reveals the throughput improvement is inversely proportional to the number of users. This is because multi-user diversity gain occurs as the number of users gets bigger; however, when the number of users is too large compared with the number of RBs, using an additional RB from a neighbouring cell for coordinated multipoint transmission will aggravate the lack of radio resources. It can be seen that the throughput of the proposed algorithm is nearly 32% larger than the static cooperation set scheme and 39% higher than non cooperation (SU-MIMO) when there are 30 users per cell. However, the system throughput improvement is less with fewer users.

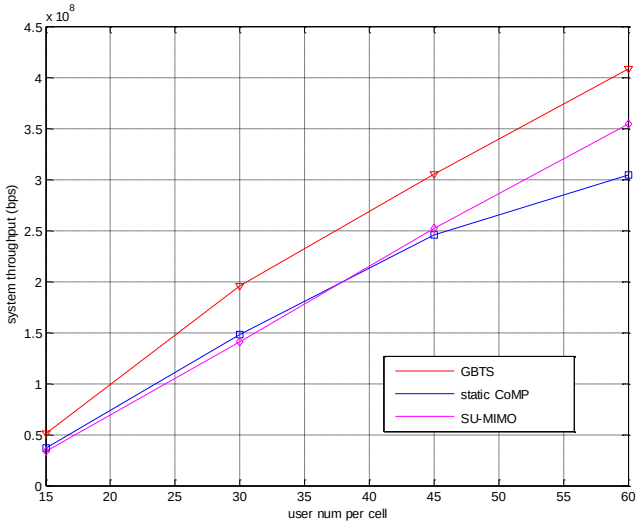

Figure 4.3 Throughput Comparison

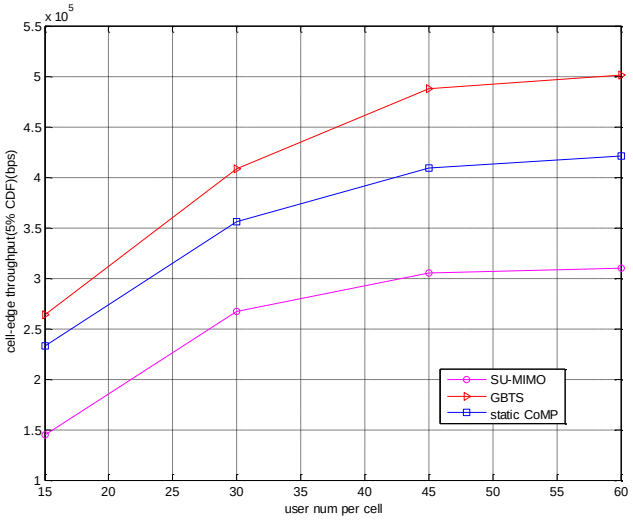

Figure 4.4 Cell-edge throughput comparison

Figure 4.4 indicates the cell-edge throughput comparison with different number of MSs. The throughput is calculated using the method of 3GPP [92] using the 5% point of the CDF curves.

The results indicate the cell-edge throughput of GBTS is higher than the cell-edge throughput of the static CoMP and SU-MIMO schemes. The reason is the CoMP schemes provide cooperation transmission for cell-edge MSs in order to improve the cell-edge performance. However, the SU-MIMO scheme only provides a direct link to cell-edge MSs. Furthermore, comparing the GBTS and static CoMP, GBTS uses a dynamic transmit antenna selection which is more adaptive than static CoMP.

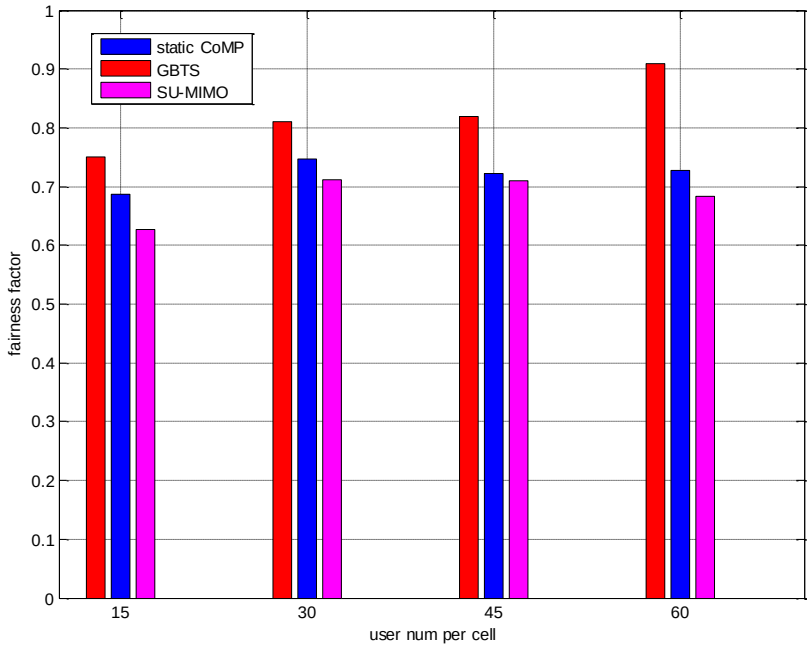

Figure 4.5 Fairness vs. Number of Users

The user fairness index with different numbers of users is shown in Figure4.5 . It can be seen that the system becomes more fair when the user number increases. That is because, the more user deployed in the system, the better user diversity achieved by the system. Furthermore, the two cooperation schemes will increase the user fairness compared with the non cooperation method. Considering the GBTS is more adaptive than the static CoMP, the fair index for GBTS is better than the static coopetive method.

4.5. Summary

In this chapter, a graph-based transmit-antenna selection method is proposed for cooperation systems. A high efficiency graph based heuristic algorithm with the concept of proportional fairness is used in the algorithm to improve the user fairness and enhance the system throughput efficiently. The simulation results indicate that system throughput is improved significantly compared with the non cooperative scheme with only a little sacrifice on fairness.

5. Inter-cell graph-based transmit antenna selection

Intra-cell cooperation can improve the system performance and cell-edge performance as shown in the chapter previously. However, the MSs may be located in the edge of the coverage area, in which case the performance of intra-cell cooperation is limited. Therefore, inter-cell cooperation is considered as it offers more opportunities for serving such users.

Inter-cell cooperation allows multiple BSs to transmit signals to multiple MSs concurrently sharing the same resource. It is specifically used for cell-edge MSs that are within the transmission ranges of multiple BSs. Since users in the cell edge region are the most prone to high ICI in OFDMA system, base station cooperation (BSC) scheme can change the interfering signal from a neighbouring base station to become part of the useful signal.

This coordination technique can significant reduce the whole system ICI to improve the cell-edge users' performance, so adding to the advantage of spatial diversity. Thus, BSC has two advantages: spatial diversity enhancement and ICI reduction.

5.1. Existing problem

The idea of BSC can be explained by Figure5.1 which gives an illustrative scenario of an ideal BSC with 3 BSs and 3 MSs.

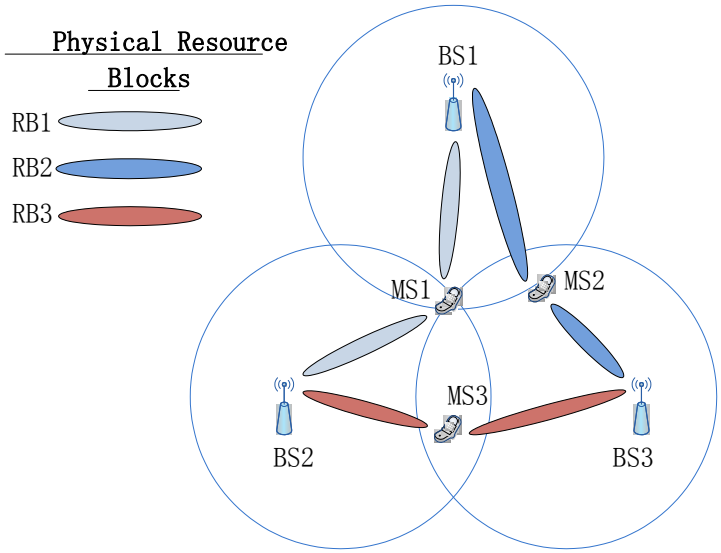

Figure 5.1 Ideal BSC cooperation

MS1, MS2 and MS3 are communicating with BS1, BS2 and BS3 respectively. The downlink signal to MS1 causes interference at MS2, and vice versa. The same issue occurs between BS1 and BS2, BS2 and BS3 respectively. However, BSC uses the inter cell interference signal as a part of the desired signal so significantly mitigating ICI [96]. However, in a practical cooperative cellular network, there are two main problems should take into consideration, which are illustrated in the next two figures.

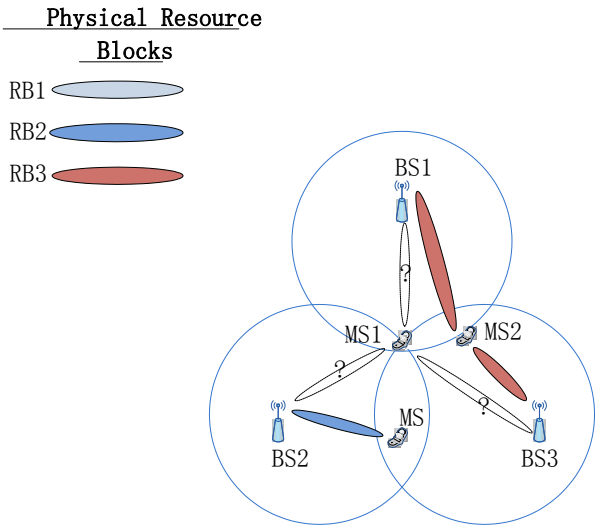

Figure 5.2 Cooperation set forming problem

How to generate the cooperative set is one such problem. In a wireless cellular network, cooperative transmission can enhance the QoS of the desired signal for a MS but will cost more RBs for the cooperative users. This may reduce the whole system spectrum efficiency. In Figure5.2, MS1 is located in the overlap region, so both BS2 and BS3 can transmit signal or interference to MS1. It is difficult to choose which BS to use for cooperation in order to make a trade-off between the signal quality and system spectrum efficiency.

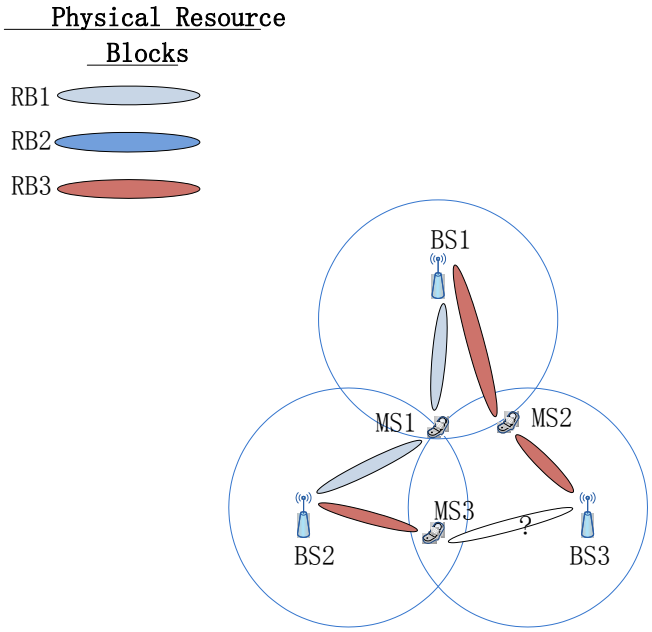

Figure 5.3 RB allocation problem

The lack of RBs is the second problem in a cooperative wireless system. Figure 5.3 reveals how such a problem may happen during RB allocation. Both MS2 and MS3 are cooperative users and are served by BS1, BS3 and BS2, BS3 respectively. In a conventional cellular network, each BS will schedule the spectrum resource individually. In this way, BS2 and BS3 may allocate RB3 to MS3 and MS2, respectively. However, BS3 then cannot allocate the same RB to MS3 in order to provide a cooperative transmission in such an allocation scheme. Therefore, a joint RB allocation scheme is required in a cooperative wireless system.

The previous problems are considered in a base station cooperation joint radio resource management scheme. The proposed algorithm optimizes the cooperative transmission efficiency and avoids the conflict on resource allocation. The main objective is to improve the cell-edge users' throughput.

5.2. Problem Formulation

The problem is decomposed into two phases.

(i) To tackle the problem shown in Figure 5.2, provision of more spatial diversity and ICI reduction is considered by choosing a proper cooperation BS. ICI is managed by using a graph theory approach.

(ii) Then, since the cooperation set is selected, a judicious resource allocation method is proposed to avoid the allocation conflict as described in Figure 5.3. The instantaneous channel quality information (CQI) is exploited in order to maximize the SINR. Reference [97] shows it is possible to have accurate CQI.

5.2.1. First Phase: Spatial diversity Enhancement and ICI Mitigation

In the first phase, an example with 4BSs and 8MSs is shown in Figure 5.4. It can infer the interference intensity from the MS's geographic location and construct a corresponding interference graph in Figure 5.5 part A). In this graph, which is denoted by $G = (\mathcal{V}, \mathcal{E})$, a node in set $\mathcal{V}$ is an MS and an edge in set $\mathcal{E}$ represents the potential interference between two MSs. e_{ij} denotes the interference between node i and node$j$. The higher the value of e_{ij} the stronger the potential interference between MS i and MS j. By calculating the e_{ij} at MS i from whole MSs j in the BS ℓ, the weight of MS i for BS ℓ can be obtained. Therefore, a graph can be constructed to indicate the relationship between BSs and MSs, which is shown in Figure5.5 part B). Every edge is assumed to have a non-negative real number. Taking two vertex sets (one for MSs and the other for BSs) Figure 5.5 part B) shows two sides of vertex sets for the case of 8 MSs and 4 BSs. The edge w_{li} represents the potential weight of interference from BS ℓ to MSi.

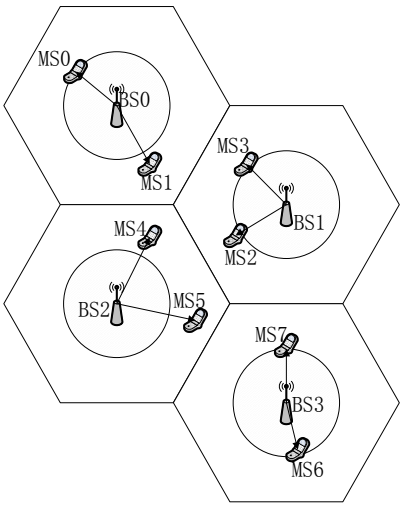

Figure 5.4 Example of a multi-cell multi-user scenario

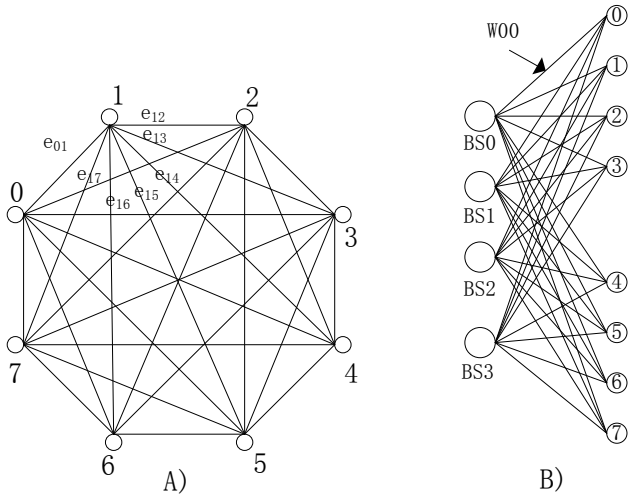

Figure 5.5 graph for multi-cell multi-user scenario

The original optimization assignment problem in graph theory is optimal assignment applicable to *weighted bipartite matching* shown in Figure 5.5part B). It is to assign n jobs to n workers. Each worker who is qualified for one or more jobs and has different efficiency for different jobs is assigned to one, or more than one, job to maximize the total efficiency. This problem was solved by the Hungarian algorithm using weighted bipartite matching graphs [98], a very famous theorem in graph theory that is described as follows:

Theorem: if a number is added to or subtracted from all of the entries of any one row or column of a cost matrix, then on optimal assignment for the resulting cost matrix is also an optimal assignment for the original cost matrix.

Here, matching corresponds to a transmission provided between BS and MS. Each MS may have more than one matching, which means more than one BS communicates to the MS simultaneously. Since the aim of the Hungarian algorithm is maximize the total $\max \sum_{l} \sum_{i} w_{li}$, the result will tend to transfer the interference channel into part of the desired signal channel, thus achieving spatial diversity enhancement and ICI mitigation.

5.2.2. Second Phase: SINR Maximization

Each MS is served by different BSs after the first-phase assignment. In the second phase, the solution focuses on the resource block allocation problem. The main goal for the second phase is to find the best resource block that maximizes the user capacity and avoids the conflict as mentioned before by putting the PBs in jointly managed pools.

For a non-cooperative user, the resource block will be selected from its own anchor cell.

For a cooperative user, the cooperative cells will select the same RB from its individual RB pools, and then using a joint scheduling algorithm among these RBs to provide the cooperation communication. Once the RB is selected, it will be wiped from the available RB pools in each cooperative cell. Note that ICI is mitigated in the first phase, so the second phase just needs to consider maximizing SINR and avoiding the conflict of resource allocation.

5.2.3. Weight Edge for First Phase

The interference weighted graph is used to evaluate the possible interference between each BS and MS. The graph is constructed in two steps.

(i) In the first step, since downlink transmission from one BS to a MS will cause interference to other MSs on the same resource block (RB), a *MS-MS* interference weighted graph is generated.

(ii) In the second step, the *MS-MS* graph is converted into *BS-MS* interference weighted graph according to the relationship between anchor BSs and MSs.

Let $G = (\mathcal{V}, \mathcal{E})$ represent the MS-MS interference weighted graph, set $\mathcal{V}$ denotes MS set and set $\mathcal{E}$ represents the possible interference set between MSs. e_{ij} denotes the interference between node i and node j. The higher the value of e_{ij} the stronger the interference is.

Table 5.1 Downlink transmission parameters

MS No.	Anchor BS	Potential Coop-BS	Position
MS0	A_0={0}	B_0={Ø}	Centre
MS1	A_1={0}	B_1={1,2}	Edge
MS2	A_2={1}	B_2={2}	Centre
MS3	A_3={1}	B_3={0}	Centre
MS4	A_4={2}	B_4={0,1}	Edge
MS5	A_5={2}	B_5={1,3}	Edge
MS6	A_6={3}	B_6={Ø}	Centre
MS7	A_7={3}	B_7={1}	Centre

An example is shown in Table 5.1 corresponding to Figure 5.2. It can infer the interference intensity between any two MSs from this table.

(i) MS0 and MS1 are both located in the same anchor cell and have severe

interference, unless allocated different RBs.

(ii) MS1 may endure heavy ICI from MS4 unless it uses base station cooperation, not only because the anchor cell of MS4 is in the diversity set of MS1 but because both MS1 and MS4 are cell-edge users.

(iii) Since the anchor cell of MS3 is in the diversity set of MS1, and MS3 is a cell-centre user, MS3 will slightly interfere with MS1 from a different cell.

(iv) Although ICI will exist between MS1 and MS6, base station cooperation cannot establish a connection from MS6's anchor cell to MS1. e.g., MS6's anchor cell is not included in MS1's diversity set.

Generally, 3 bits of information are needed to construct the graph: 1 bit to indicate whether the two BSs have the same anchor cell; 1 bit to show whether the two MSs have the same elements in each diversity set; 1 bit to indicate whether the MS is cell-edge.

Since each BS knows its registered MS, the bit to show whether the two MSs have the same anchor cell is not necessary on the signalling exchanging between BSs. Therefore, only 2 bits are required for the signalling exchange between BSs to represent the interference weight value between two MSs.

Define e_s as the weight associated with the no possible cooperation (intra-cell interference). e_0, e_1, e_2 correspond to the weights of possible base station cooperation depending on the geographic location of the two MSs:

(i) e_0 (weakest ICI) denotes the weight of the possible cooperation between two centre MSs;

(ii) e_1 (medium ICI) denotes the weight of a possible cooperation if one is a cell-edge user and the other one is a centre user;

(iii) e_2 (severe ICI) denotes the weight of a possible cooperation between two cell-edge users.

(iv) e_N denotes the weight associated with inter-cell interference in the same diversity set.

As a result, the five weight values (including intra-cell interference) can be sorted as

$$e_N \ll e_0 < e_1 < e_2 \ll e_s \tag{6.2}$$

Inter-cell interference e_N will inflict the smallest damage; the system can accept interference at such a level. Inter-cell interference e_0, e_1, e_2 will depend on the system requirement to choose whether to endure the interference or provide base station cooperation. Since the intra-cell interference e_s is the largest interference, different RBs need to be assigned to avoid the interference. The weight evaluation procedure is given as follows:

e_s should be significantly large such that

$$\forall \delta > 0, \exists N \in \mathbb{Z}^+, \forall n > N \Rightarrow \quad n(e_s - e_2) - e_s > \delta \tag{6.3}$$

The procedure of the interference weighted graph construction is:

Step 1: Initialize all edges let $e_{ij} = 0$.

Step 2: For each user i and user j, if $A_i \cap A_j \neq \varnothing$, let $e_{ij} = e_s$, otherwise, go to step 3.

Step 3: If $A_i \cap B_j \neq \varnothing$, go to step 4, otherwise, let $e_{ij} = e_n$

Step 4: If both user i and user j are cell-edge users, let $e_{ij} = e_2$, else if one is

cell-edge user and the other one is centre user, let $e_{ij} = e_1$, else if both user i and user j are centre users, let $e_{ij} = e_0$.

Step 5: Update e_{ij}

Since the weight e_{ij} for each two users is determined, it is possible to infer the possible interference level denotes as w_{nj} between BS *n* and user *j*, such as

$$w_{ni} = \sum_{A_j = n} e_{ij} \tag{6.4}$$

The interference weighted graph for Table 6.1 is illustrated in Figure5.4, where each edge connected between BS and MS contains an interference weight.

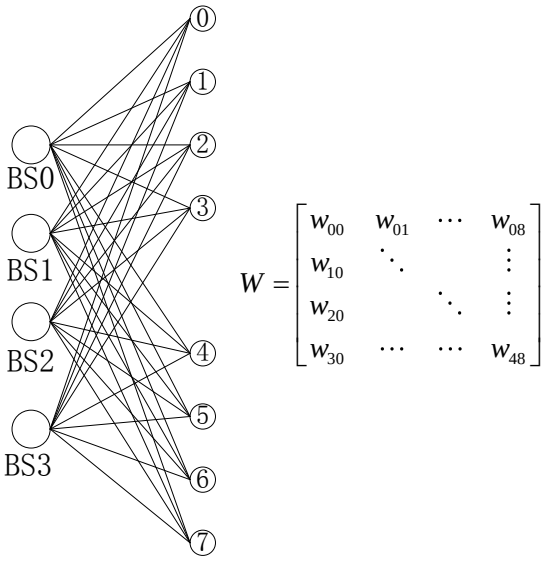

Figure 5.6 Interference weighted graph

The generated matrix is illustrated by the weight between any pair of BS to MS, which will be used in the next section.

5.3. Cooperation Set Selection Algorithm

In this section, a new algorithm called Graph-Based Dynamic Coordinated

Clustering algorithm is proposed for clustering the cooperation set for each user based on large-scale fading. This allocation algorithm tries to find the optimal user-cell matching for the weighted matrix, taking a graph theoretical approach.

5.3.1. Solution of Dynamic Coordinated Clustering

An overhead-exchange-limited dynamic coordinated clustering scheme is proposed to mitigate the ICI effect. Since the higher value of w_{nj} corresponds to the higher channel gain between BS n and MS j, the basic idea of a coordinated clustering scheme is to assign the MSs to BSs with higher value of w_{nj} in order to provide the BSC more efficiently. Therefore, there is a close relationship between the coordinated clustering scheme and the Hungarian Algorithm (HA) [98]. However, the HA is used to solve a one-to-one match, so in this case the HA has been modified into a many-to-many case.

The dynamic coordinated cluster is generated under two constraints: (i) the size of coordinated cluster; (ii) the limitation of available RBs. Denote $\mathcal{N}_{\mathrm{coop}}$ and $\mathcal{N}_{\mathrm{RB}}$ as the size of coordinated cluster and number of available RBs per sector respectively. Define ρ_{nm} as a binary value, where if $w_{nj} = 0$ then $\rho_{nj} = 1$, otherwise, $\rho_{nj} = 0$. Matrix $\mathrm{W} = [w_{nj}]$ is composed of weight w_{nj}, which are shown Figure5.6. The proposed algorithm tries to find a coordinated cluster for each user iteratively. The procedure is described below:

5.3.2. Process of Dynamic Coordinated Clustering

Step 1: Initialize two labels a_{n} and b_j by

$$a_n = max\,[w_{0j}, \dots, w_{nj}]\,, b_j = 0\,, i \in 1 \cdots \mathcal{M}$$

Step 2: Obtain the excess matrix C by the following.

$$\begin{cases} c_{nj} = 0 & if\ w_{nj}\ marked\ by\ symbol * \\ c_{nj} = a_n + b_j - w_{nj} & otherwise \end{cases}$$

Step 3: Find the subgraph G that includes vertices n and j satisfying $c_{nj} = 0$ and the corresponding edge w_{nj}. Then, find the matching following

For each row:

$$\begin{cases} a_{nj} = a_n - 1, & (\sum_j \rho_{nj \le \mathcal{N}_{RB}}) \\ a_n = a_n, & (\sum_j \rho_{nj > \mathcal{N}_{RB}}) \end{cases}$$

If $\sum_j \rho_{w_{nj \le \mathcal{N}_{RB}}}$, then mark the row with a $\triangle$.

For each column

$$b_j = b_j + 1, (\sum_n \rho_{nj \le \mathcal{N}_{COOP}})$$

Step 4: If each row is marked by $\triangle$, then go to step 5, otherwise return step 2.

Step 5: For each element, c_{nj} is marked by $*$ only under the following condition, (i) $c_{nj} = 0$; (ii) the number of marked element in the row is smaller than $\mathcal{N}_{RB}$, i.e., each BS cannot allocates more than its can serve; (iii) the number of marked elements in the column is smaller than $\mathcal{N}_{coop}$, i.e., each MS cannot be served by more than the required number of cooperative BS.

Step 6 The elements c_{nj} marked by $*$ denote the MS j served by BS n. Matrix $\mathcal{C}$ is the suboptimal assignment solution

5.3.3. Properties of the algorithm

The cooperation set selection algorithm has useful properties:

Property 1: An MS can be only connected with other BSs - at most N_{coop} BSs.

Property 2: Any MSs will be served by its anchor BS.

Property 3: The number of available RBs should be larger or equal than the maximum size of the cooperative set.

5.4. Radio Resource Management Algorithm

In the previous section, a cooperation set matrix C is generated with two constraints: (i) the size of cooperation set; and (ii) the limitation of available physical radio resource. A heuristic algorithm is proposed in this section to avoid the resource conflict during radio resource allocation.

After the first-phase partition, MSs are distributed into their cooperative set. In the second phase, it is necessary to decide which RBs will be allocated to which user. Since there are N_{RB} resource blocks in each cell, $N_{rb}!$ possible choices exist in radio resource allocation, which is computationally infeasible. Here a heuristic suboptimal algorithm is proposed that iteratively assigns RBs to BSs.

This is as follows:

Step 1: Initialize the RB pool for each BS.

Step 2: For each RB pool, sort the weighted, which is calculated by the Shannon capacity, in descending order.

Step 3: for each user, assigned the assign the RB with the maximum weight in the RB pool.

Step 4: Update the available RB set by deleted the assigned RB.

Step 5: Repeat step 2-4 for all nodes.

5.5. Performance Simulation and Analysis

In this section, the performance of the proposed schemes is evaluated. Four sample values are used with different quantized methods and thresholds to examine the system performance with different weighted values for each edge, which is shown in

Table 5.2, the results show the simulation result of sample 3 is better than others; this is given by $(e_N, e_0, e_1, e_2, e_s) = (0,25,50,100, 10^3)$

It should be noted that the proposed algorithm is not very sensitive to the chosen weight values and the size of coordinated cluster. Thus, the algorithm could be used in different situations with different service requirements.

Table 5.2 evaluation of system parameters

	Sample1	Sample2	Sample3	Sample4
Throughput (10^8 bps)	1.65	1.63	1.79	1.69

Three schemes were tested in a scenario with 30% cell-edge users for three different schemes: (i) the proposed dynamic coordinated clustering scheme, (ii) a static clustering scheme and (iii) a non-BSC scheme.

Figure 5.7 indicates the system throughput versus number of users. Since using an additional RB from a cell to provide cooperation will aggravate the lack of RBs, the system throughput of the proposed scheme is lower than the non-BSC system, but better than the static clustering scheme. However, the system throughput of the proposed scheme is higher than the non-BSC scheme when the number of users per sector is small. That is because, since the number of users per sector is small, there are more RBs that can be used to provide cooperation and RB-starvation is not an issue.

Figure 5.8 show the cell-edge throughput with different users per sector. The simulation result indicates the proposed dynamic clustering scheme has the highest cell-edge throughput compared with the static clustering scheme and the non-BSC scheme.

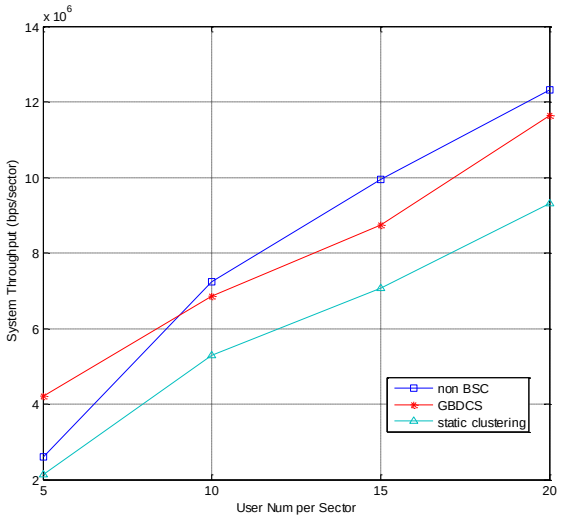

Figure 5.7 System throughput with different user per sector

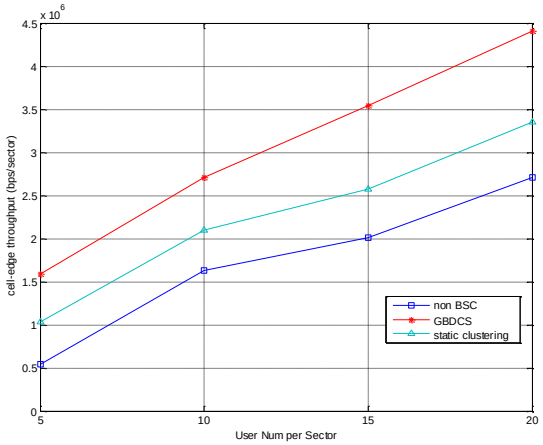

Figure 5.8 Cell-edge throughput with different user per sector

Figure 5.9 and Figure 5.10 show the system throughput with different percentages of cell cell-edge users under different traffic load (with 20 and 5 distributed MSs per sector respectively). When all users are cell centre users, no cooperative transmission happens (as 0% cell-edge users) and the frequency of cooperative transmission is proportional to the percentage of cell-edge users. Therefore, the cooperative gain increases when the percentage of cell-edge users increases. In the heavy traffic load scenario, Figure 5.9 indicates that the throughput of the proposed scheme is higher

than the static clustering scheme. That is because the proposed dynamic clustering scheme is more flexible and can mitigate the inter-cluster interference. Considering the lack of RBs, the proposed scheme has a lower system throughput than the non BSC scheme when the percentage of cell-edge users is small. However, when there are more cell-edge users, more users endure the severe inter-cell interference, so the throughput of the proposed scheme becomes higher than the non-BSC – in this example when the proportion of cell-edge users is larger than 40%.

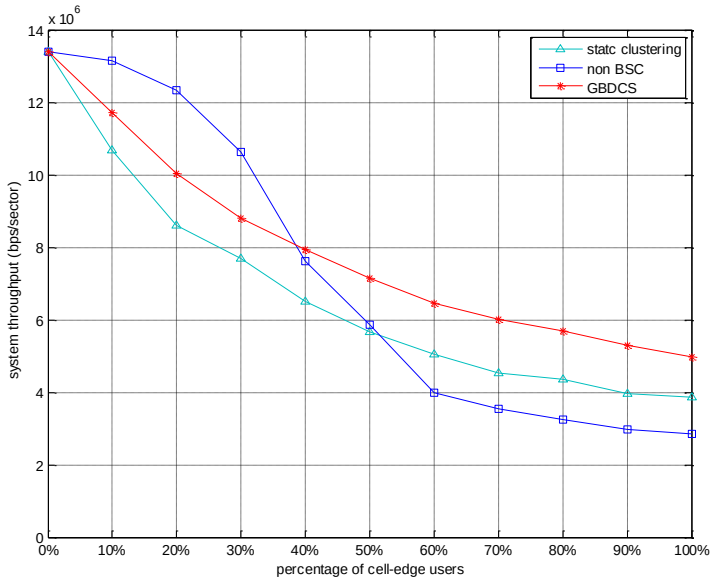

Figure 5.9 system throughput with 20 users per sector

In Figure 5.10, as there are sufficient RBs in a light traffic scenario, the throughput of the proposed scheme is higher than the non-BSC scheme and the static clustering scheme.

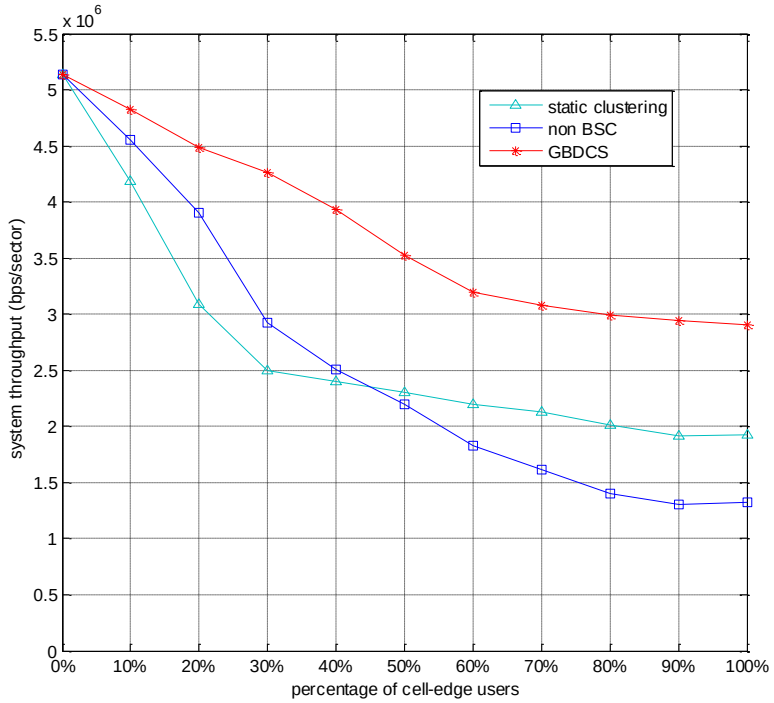

Figure 5.10 system throughput with 5 user per sector

The distribution function for the SINR is shown in Figure 5.11. The solid line denotes the distribution of SINR for the BSC scheme and the dashed line for non-BSC. In Figure 5.11 it can be seen the non-BSC scheme has a much larger probability of having a low SINR (from -20dB to 3dB). In addition, the probability of the SINR for the BSC scheme being in the middle range (from 4dB to 25dB) is larger than for the non-BSC scheme because the cell-edge users always suffer a high level of interference in the conventional system. The BSC scheme prefers to choose cell-edge users as cooperative users. Therefore, most of the cell-edge users see their SINR improved from a low level to the middle level. The two schemes have nearly the same probability for the high SINR area (26dB to 40dB). This is because users can always achieve a high SINR performance at the cell-centre (so the cell-centre users are always picked as non-cooperative users in BSC scheme). Therefore, the BSC scheme adds little contribution at high level SINR area.

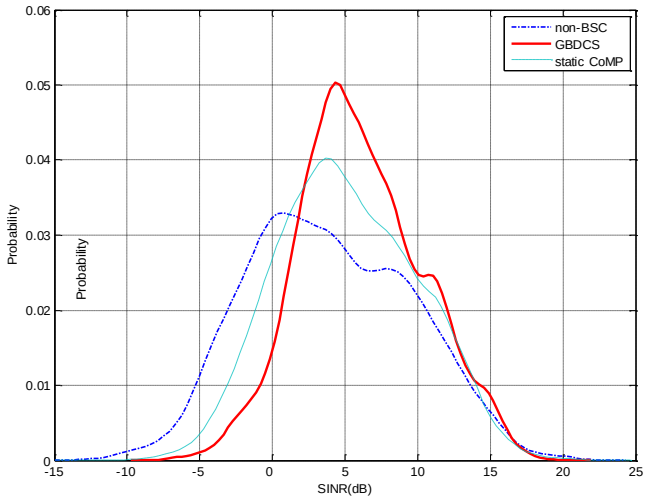

Figure 5.11 Distribution comparison of SINR

5.6. Summary

In this chapter, a novel dynamic coordinated clustering scheme in a wireless BSC network was presented. Considering the feasibility of information exchange, coordinated clusters are generated with only 2bits signalling exchange between BSs. The simulation results show the proposed scheme can improve the performance of cell-edge users compared with the non-BSC scheme and the static clustering scheme.

6. Cross-Layer Cooperative transmission scheme

6.1. Introduction

In traditional cooperative wireless network, multiple BS will provide a transmission service to one MS under the same RB. While a cooperative clustering algorithm in the MAC layer can enhance the quality of the desired signal at a cost of a reduction in the system spectrum efficiency, improved coding in the PHY layer can overcome the problem of a reduction in the system spectrum efficiency.

By utilizing the cooperative coding scheme, two transmitters could operate in a cooperative way in order to transmit the signal to two individual MSs with signal enhancement and interference mitigation. However, it is hard for a PHY layer cooperative scheme to decide how to generate a cooperative cluster, but this is exactly what the MAC layer cooperative scheme does.

Combining the MAC layer and PHY layer schemes as a cross-layer cooperative scheme maximises the system performance.

This is done as follows:

(i) The cross-layer cooperative scheme generates the cooperative clusters

(ii) After the cluster is formed, the traditional 802.11n coding scheme is used for the non-cooperative MSs and a cooperative coding scheme for the cooperative MSs.

It is noted that, as an inter-cell cooperation scenario is considered, the cross-layer scheme uses the algorithm described in chapter 5.

The optimization target is increasing the cell-edge user's throughput in a MU-MIMO scenario. For a MU-MIMO system, allocating the same resource blocks to different users would increase the sum-rate capacity so this is investigated in the PHY layer.

6.2. PHY Layer cooperative coding scheme

In the previous chapter, an inter-cell cooperation scheme is proposed to indicate the cell-edge performance improved as a cost of the system spectrum efficiency. To tackle this problem, a new cooperative coding scheme is proposed to increase the data rate to thereby improve the system spectrum efficiency. This chapter considers a new achievable rate region for interference channels with transmitter cooperation.

The classic interference channel (IC) model is a two-sender and two-receiver model, that was introduced in [99][100]. In this model, each transmitter sends information to the corresponding receiver and interferes with the other transmitter-receiver pair. The study of the interference channel is important for communication system design, because practical systems are designed to operate in the interference scenario. In [101], Han and Kobayashi proposed the now famous achievable rate region for the interference channel, where the message is split into common information and private information. This splitting technique is used to partially decode and subtract the interfering signal.

Due to the scarcity of the spectrum resource and high data transmission requirement, the inter-cell interference (ICI) has now become a bottle-neck problem limiting the system performance [100]. Cooperative transmission has drawn much research attention [103][104][105] to not only mitigate the interference but also to improve the desired signal strength.

IC with degraded message sets (IC-DMS) was proposed in [106]. By utilizing cognitive techniques, the cognitive transmitter gains full knowledge of another transmitter's message. The two transmitters send information to the corresponding receiver associated with it. In this scenario, the cognitive transmitter-receiver pair with Gel'fand-Pinsker coding [107] exploits the cooperation to improve the overall system performance. In [108][109], different coding schemes were proposed to derive a new achievable rate region; these references prove a capacity-achieving scheme for

the Gaussian IC-DMS (GIC-DMS) in the low interference regime, in which the cross link gain between receiver and interfering transmitter is less than or equal to 1. As the coding scheme in [108][109] is non-optimal for GIC-DMS in a high interference regime, a new coding scheme was proposed in [110] to overcome the drawbacks. The scheme in [111] with finite-rate cooperation at transmitters improves the achievable rate region in both the low and high interference regimes. In [112], the achievable rate region is studied with user cooperation.

However, most of the schemes focus on sharing the public information at either transmitter or receiver in order to subtract the interference. In this chapter, a new cooperation scheme is introduced in order to improve the signal strength with interference *avoidance*. One side information cooperation is used at the transmitter with a finite-rate constraint and a new achievable rate region is characterized to demonstrate the improvement in sum rate.

For a two-transmitter, two-receiver interference channel in a cooperative scenario, assume transmitter S_1 has knowledge of the message to be transmitted by S_2. Once S_1 has S_2's message, two possible coding techniques are possible:

i) S_1 treats the message of S_2 as interference and tries to compensate for it by using Gel'fand and Pinsker's coding scheme [102]. This results in an achievable region for the rate pair that enlarges the region in [101], and reduces to that region for the case where no interference mitigation is performed. An example is given in the Figure 6.1 a).

ii) S_1 could refrain from transmitting its own information and act as a relay for S_2. In this case, a 2 transmitter to 1 receiver multiple-input single-output channel between $(S_1, S_2) \rightarrow \mathcal{R}_1$ is obtained [103]. An example is given in Figure 6.1 b).

The main results in [100] show that time sharing can achieve the convex hull of the

regions obtained using these two coding techniques. The first coding scheme aims to mitigate the impact of interference. However, the second scheme tries to increase the signal strength for cooperative users without considering the direct-link users. In this chapter, a coding scheme with transmitter cooperation is introduced in order to not only minimize the impact of interference for directly user but also strength the signal for cooperative user.

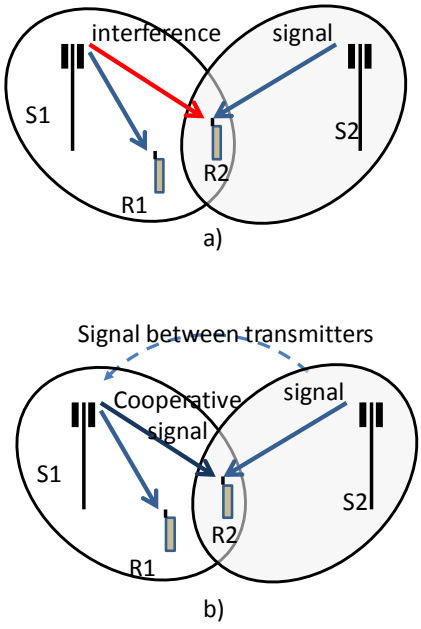

Figure 6.1 Interference channel model with transmitter cooperation

6.2.1. System Model

A finite rate link between transmitter 2 (S2) and transmitter 1 (S1) is deployed and the relation between the two senders is asymmetric. This is a reasonable interference channel model for the target application of transmitter cooperation in which one sender is transmitting and the second sender obtains the first sender's transmission before starting its own. Therefore, S_1 has knowledge of the message to be transmitted by S_2 so S_1 can then exploit the knowledge of S_2's message to provide cooperation transmission, and potentially improve the transmission rate.

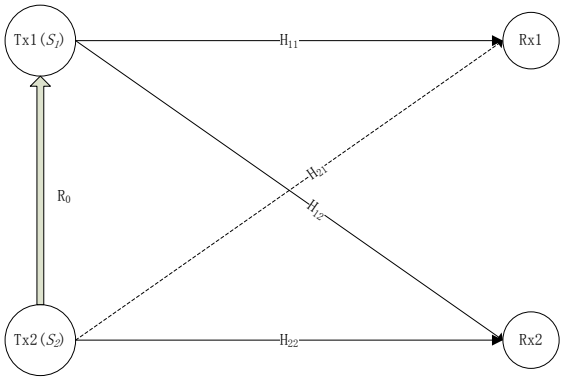

Figure 6.2 Interference channel model with transmitter cooperation

An *(n, K_1, K_2,ε) code* for the interference channel with cooperative transmission consists of K_2 codewords $x_2^n(j) \in \mathcal{X}_2^n$ for S_2, and $K_1 \cdot K_2$ codewords $x_1^n(i,j) \in \mathcal{X}_1^n$ for S_1, $i \in \{1,2,\cdots K_1\}, j \in \{1,2,\cdots K_2\}$, which together form the *codebook*, revealed to both senders and receivers such that the average error probabilities under some decoding scheme are less than ε. A rate pair *(R_1, R_2)* is said to be *achievable* for the interference channel with cooperative transmission if there exists a sequence of *(n,* $2^{[nR_1]}, 2^{[nR_2]}, \varepsilon_n$*)* codes such that $\varepsilon_n \to \infty$ as $n \to \infty$. An achievable region is a closed subset of the positive quadrant of $\mathbb{R}^2$ of achievable rate pairs [103].

The interference channel capacity region, in the most general case, is still an open problem; this is the case for IC-DMS as well. In [101], the achievable region of the IC is found by first considering a modified IC and then establishing a correspondence between the achievable rates of the modified and the original problems. A similar modification is made in the next section.

6.2.2. Modified IC with Cooperative Transmission

Similarly to [100], a modified IC with cooperative transmission C^m is introduced in this research, and demonstrates an achievable region $\mathcal{R}^m$. After that, a relation between an achievable rate for C^m and an achievable rate for C is used to establish an achievable region for the IC with cooperative transmission. The modified C^m is

defined as in Figure 6.3

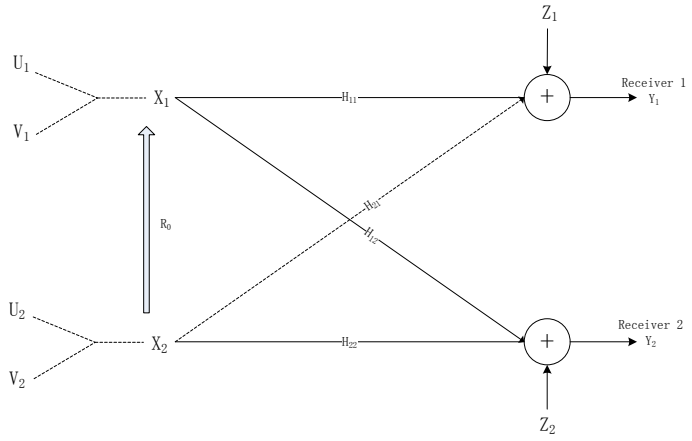

Figure 6.3 Modified interference channel model with transmitter cooperation

Let $X_1 \in \mathcal{X}_1$ and $X_2 \in \mathcal{X}_2$ be the random-variable inputs to the channel. Let $Y_1 \in \mathcal{Y}_1$ and $Y_2 \in \mathcal{Y}_2$ be the random-variable outputs of the channel. The conditional probabilities of the discrete memoryless channel are the same as in [100] and can be fully described by $p(y_1|x_1, x_2)$, and $p(y_2|x_1, x_2)$ for all values $X_1 \in \mathcal{X}_1$, $X_2 \in \mathcal{X}_2$, $Y_1 \in \mathcal{Y}_1$, $Y_2 \in \mathcal{Y}_2$.

The modified IC with cooperative transmission introduces two pairs of auxiliary random variables: (U_1, V_1) and (U_2, V_2). In this work, U_1, U_2 denote the private message sending to the corresponding receivers. V_2 denotes the public message sending to the two receivers. The message V_1 is generated to sending message to receive 2 cooperatively.

6.2.3. Cooperative Coding Scheme

The basic idea of the cooperative coding scheme (CCS) is that it is deployed as a conferencing link between two transmitters. Since S_1 receives the information from S_2 before the transmission, S_1 can transmit its own signal to R_1 and treats the message from S_2 as interference and tries to compensate for it. Furthermore, due to S_1 acknowledging the message from S_2, it can transmit the desired message to R_2 with

S_2 cooperatively. The detail of encoding and decoding are given in the appendix I.

6.2.4. Numerical results for CCS

The achievable rate region is used in this section in order to evaluate the performance in theoretically. For a Gaussian channel scenario, in the weak interference regime where a_{21}, $b_{12}<1$, the achievable rate region simplifies to

$$\begin{cases} R_1 \le \gamma\left(\dfrac{\alpha P_1}{N_1 + a_{21}\beta P_2}\right) \\ R_2 \le \min\left\{\gamma\left(\dfrac{b_{12}P_1 + P_2}{N_2}\right) + R_0, \gamma\left(\dfrac{b_{12}\bar{\alpha}P_1 + \beta P_2}{N_2 + b_{12}\alpha P_1}\right) + \gamma\left(\dfrac{a_{21}\bar{\beta}P_2}{N_1 + a_{21}\beta P_2 + \alpha P_1}\right) + R_0\right\} \end{cases} \tag{6.1}$$

In the strong interference and strong cooperation scenario where a_{21}, $b_{12}>1$, the achievable rate region simplifies to

$$\begin{cases} R_1 \le \gamma\left(\dfrac{P_1}{N_1}\right) \\ R_2 \le \gamma\left(\dfrac{b_{12}P_1 + P_2}{N_2}\right) + R_0 \\ R_1 + R_2 \le \gamma\left(\dfrac{a_{21}P_2}{N_1}\right) + \gamma\left(\dfrac{b_{12}P_1}{N_2}\right) + R_0 \end{cases} \tag{6.2}$$

This derivation given achievable rate regions for regimes a_{21}, $b_{12}<1$ and a_{21}, $b_{12}>1$ as in (6.1) and (6.2) are shown in appendix II.

Figure 6.4 shows the achievable rate region of a Gaussian IC in the weak interference regime, with $P_1=P_2=6$, $a_{21}=b_{12}=0.55$. The red line denotes the classic Han Kobayashi common-private power splitting scheme, and the blue line denotes the IC with transmitter cooperation. The cooperation improves the performance of R_2 at the expense of the rate for R_1. That is because Tx_1 needs more transmit power to the cooperative receiver Rx_2 instead of the direct link receiver Rx_1.

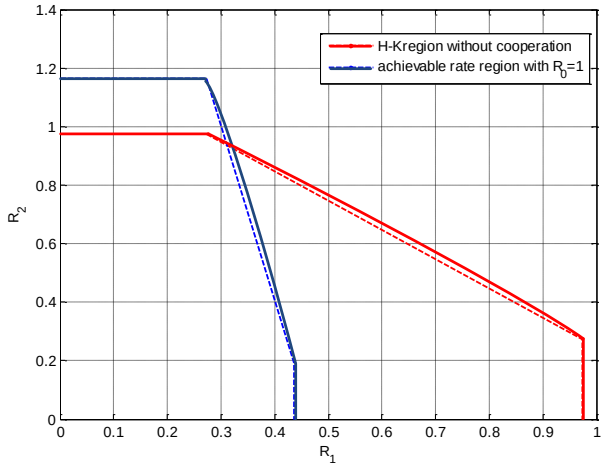

Figure 6.4 Achievable rate region for weak interference with $P_1=P_2=6$, $a_{21}=b_{12}=0.55$

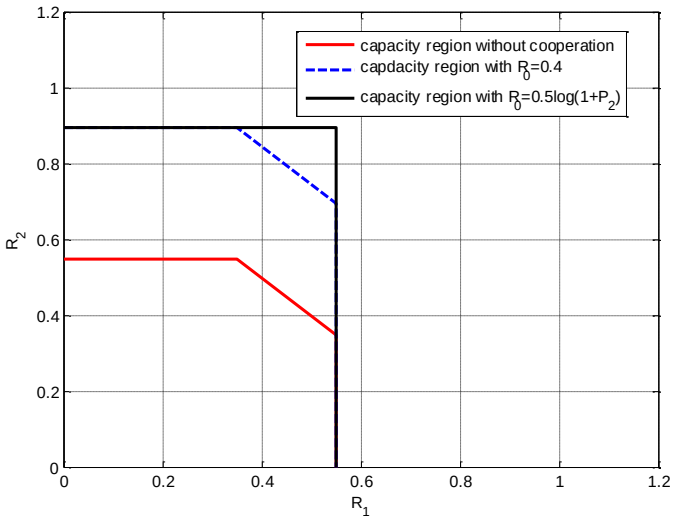

Figure 6.5 Achievable rate region for strong interference with $P_1=P_2=2$, $a_{21}=b_{12}=1.5$

In the strong interference regime, the capacity region of IC with transmitter cooperation is achieved by transmitting only at the cross link. i.e., the private message from Tx_1 to Rx_2, and the common message from Tx_2 to Rx_1. In the strong interference scenario, the cooperation link increases the capacity by helping the decoding of the private information at Rx_2. In fact, a conferencing link R_0 increases the sum capacity by exactly R_0. As a numerical result, Figure 6.5 illustrates the

capacity region of an IC with transmitter cooperation in a strong interference regime with and without cooperation. The channel parameters are set to be $P_1=P_2=2$, $a_{21}=b_{12}=1.5$. The results indicate the achievable rate region increases when R_0 increase. The capacity region without cooperation (H-K scheme) is the red pentagon. The capacity expands to the blue pentagon region with cooperation and $R_0=0.4$. If $R_0 \geq \frac{1}{2}\log(1+P_2)$, the Tx_1 can be fully cooperative with Rx_2, in which case the achievable rate region becomes the black rectangle.

6.3. Cross-Layer cooperative strategy

In the earlier chapter, an individual technique for increasing the cell-edge system throughput and improving the user fairness is proposed: in chapter 4, an inner-cell transmit antenna selection algorithm is proposed focusing on system throughput with user fairness; in chapter 5, a novel inter-cell graph-based transmit antenna selection algorithm is proposed with emphasising the cell-edge throughput improvement with a cost of the whole system throughput, and a judicious RB allocation method is given in order to avoid the RB conflict during cooperation. In this chapter, to focus on improving cell-edge users' performance, a cross-layer scheme is proposed with a combination of the schemes proposed in chapter 5 and chapter 6. It is noted that, in a multi-cell scenario, the system performance can also benefit by combing the schemes proposed in chapter 5 and PHY layer, the combination can be seen as a traditional MU-MIMO system. Since the cooperation may not only happen intra-cell but also inter-cell, the cross-layer scheme here only combines the inter-cell cooperation for MAC layer and cooperative coding scheme for PHY layer.

The details of comparisons are shown in Table 6.1 and described in the following:

Table 6.1 Downlink transmission parameters

Scheme number	Joint algorithm name	Coding scheme	RB allocation	Serving cell selection
1	MIMO	802.11n	PF	Max SINR
2	MU-MIMO	DPC	PF	Max SINR
3	static CoMP	802.11n	Dynamic allocation	static clustering
4	static MU-CoMP	CCS	dynamic allocation	static clustering
5	GB-DCS	802.11n	Dynamic allocation	DCS
6	GB-MU-DCS	CCS	Dynamic allocation	DCS

(1) can be seen as a traditional single user MIMO scenario, the classic modulation and coding scheme proposed in the 802.11n standard being used. The scheduling algorithm is proportional fairness, and the serving cell selection is based on the max SINR. For

(2) is effectively a traditional multi-user MIMO scenario, with the dirty paper coding scheme deployed in the PHY layer, with the same scheduling scheme and serving cell selection scheme used as in (1).

(3)-(6) consider a cooperation scenario, so that a joint scheduling algorithm proposed in chapter 5 is deployed. For the single user scenarios, (3) and (5), the classic coding scheme is used as in (1). For the multi-user scenarios, (4) and (6), the cooperative coding scheme proposed in this chapter is deployed in the PHY layer instead. Static CoMP, (3) and 4), generates the cooperative set according to that in [93]. For (5) and (6), the dynamic cooperative set selection scheme in chapter 5 is deployed.

6.4. Simulation Result and Analysis

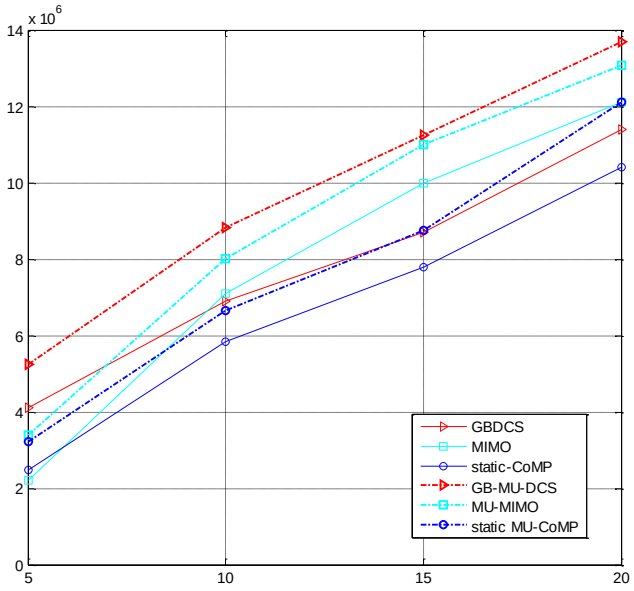

Figure 6.6 System throughput vs. user number

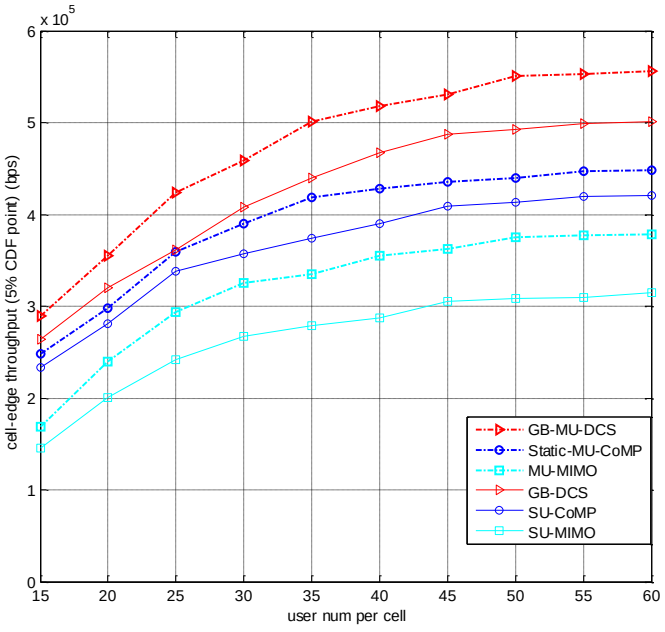

Figure 6.7 Cell-edge throughput vs. user number

Figure 6.6 indicates the cooperative scheme always has higher throughput for

cell-edge users. In the single user scenario, using an additional RB from a cell to provide cooperation will aggravate the lack of RBs, so the system throughput of the proposed scheme is lower than the non-cooperative system, but better than the static clustering scheme. However, the system throughput of the proposed scheme is higher than the non-BSC scheme when the number of users per sector is small. Under this condition there are more RBs that can be used to provide cooperation.

In the multi-user scenario, the proposed system throughput has the best performance compared with the other two due to the exploitation of multi user diversity in the system. Figure 6.7 shows the cell-edge throughput with different users per sector. The simulation result indicates that the proposed dynamic clustering scheme has the highest cell-edge throughput compared with the static clustering scheme and the non-BSC scheme both in MU and SU system.

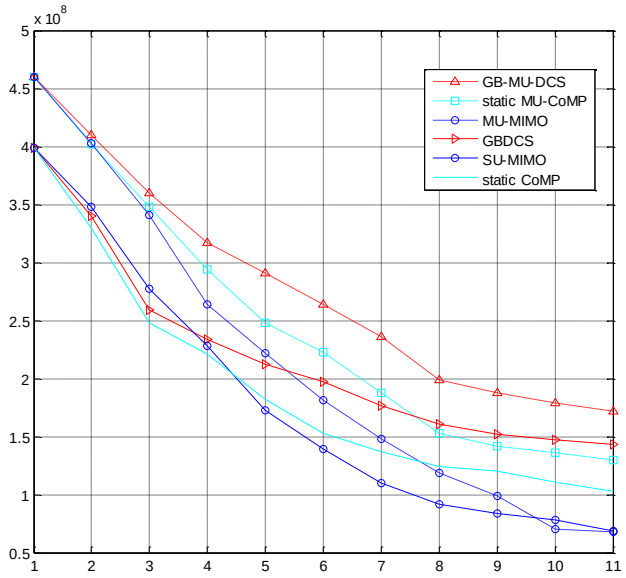

Figure 6.8 System throughput vs. percentage of cell-edge users

Figure 6.8 shows the system throughput compared with different percentages of cell-edge users. It indicates that multi-user systems always have a better performance compared with the single-user systems.

The throughputs for cooperative schemes are lower than non-cooperative schemes when there are few cell-edge users in the single-user system, but higher for larger numbers. Because of multi-user diversity, the throughputs for cooperative schemes are always better than non-cooperative users.

6.5. Conclusion

In this chapter, a dynamic coordinated clustering scheme in a wireless base station cooperation network is presented. Considering the feasibility of information exchange, coordinated clusters are generated with only 2bits signalling exchange between BSs. The simulation results show the proposed scheme can improve the performance of cell-edge users compared with the non-BSC scheme and the static clustering scheme.

7. Conclusions

This thesis describes research on cooperation strategy in OFDM based cellular networks; the aim of this research is to improve the cell-edge throughput, mitigate the inter-cell interference impact and improve the user fairness.

Generally, cooperation in the MAC layer can significantly increase the cell-edge throughput with limited signalling exchange, but at expense of the overall spectrum efficiency. However, cooperation in the PHY layer can improve the cell-edge throughput without affecting the sum rate capacity. Therefore, cross-layer cooperation becomes a possible solution for the next generation wireless system.

In this chapter, the major research contributions are summarized and possible further research work is discussed at the end.

7.1. Research Contributions

This research deployed a cooperative technique in both the PHY and MAC layers in order to mitigate the inter-cell interference. Specifically, the main contributions of this research are:

(i) A cooperative coding scheme with private information sharing:

- A rate-limited link is considered in an interference channel model and new achievable rate region is derived under different interference scenarios, showing the sum-rate capacity has increased.

(ii) A transmit antenna selection algorithm that considers the available resource block and user fairness for throughput improvement:

- The results reported in the thesis show the algorithm can achieve a better fairness than the traditional antenna selection algorithm in typical distribution scenarios.

(iii) A cooperative clustering approach based on graph theory that considers cooperative resource allocation and limited signalling exchange:

- The results indicate that the cell-edge throughput is improved compared with static clustering and traditional wireless cellular networks under different traffic load scenarios.

(iv) An assessment of combining the different techniques to allow cross layer cooperation:

- This combination allows multi user cooperative transmission to overcome the shortcomings in individual approaches.

- The results show the combination can improve both system throughput and cell-edge users' throughput without spectrum efficiency impact.

7.2. Future Work

In this thesis, cooperation technique is studied in both the PHY and MAC layers and appropriate algorithms can significantly improve system throughput and reduce inter-cell interference without occupying too much spectrum resource.

Although the cooperative techniques have proved to improve the system performance, the wireless cellular network still poses many research challenges to cooperative performance. Research could investigate the following in the future:

- All the algorithms are considered in the downlink; this could be extended to the uplink

- Cooperation for different QoS service can be considered as an extension.

- The algorithm can be extended to relay based wireless scenarios.

Meanwhile, there are other relevant techniques can improve the performance,

particularly for those cooperative users. One such technique is potential cooperative set designing. A proper potential cooperative set can significant reduce the signalling exchange and enhance the precision of cooperative set selection. Precoding is another important way to mitigate interference impact and improve the system performance, so this is an area that should be studied as a next stage work.

8. References

[1] 3GPP TS 36.423 V8.8.0, "Evolved universal terrestrial radio access network (E-UTRAN): X2 application protocol (X2AP)," Dec. 2009.

[2] 3GPP R1-060877, "Frequency domain scheduling for E-UTRA,", Mar. 2006.

[3] H. Jin, X. Wang, H. Yu, "C-MAC: a MAC protocol supporting cooperation in wireless LANs," *Wireless Communications and Networking Conference, 2009, WCNC*, 2009. *IEEE,* pp.1-6, April 2009.

[4] Benny Bing, *Broadband Wireless Access*, Kluwer Academic Publisher, 2000.

[5] Yan Zhang, Hsiao-Hwa Chen, Mohsen Guizani, *Cooperative Wireless Communications*, Auerbach Publications, 2009.

[6] I. Emre Telatar and D. Tse, "Capacity and mutual information of broadband multipath fading channels," *Information Theory, 1998. Proceedings. 1998 IEEE International Symposium on*, pp.395, Aug. 1998.

[7] B. Chen and G. Wornell, "Achieving performance of digital watermarking systems," *Multimedia Computer Systems, IEEE*, pp. 13–18, Jun. 1999.

[8] A. Nosratinia, T.E. Hunter, and A. Hedayat, "Cooperative communication in wireless Networks," *Communications Magazine, IEEE,* vol. 42, pp. 74–80, Oct. 2004.

[9] Haas, Z.J.; Tuan-Che Chen; , "Cluster-based cooperative communication with network coding in wireless networks," *Military Communications Conference, 2010, MILCOM 2010*, pp.2082-2089, Nov. 2010.

[10] Christopher, *An Introduction to LTE: LTE, LTE-Advanced, SAE and 4G mobile Communications,* John Wiley & Sons, Ltd., Publication, 2012.

[11] Catreux S., Driessen P.F., Greenstein L.J. "Simulation results for an interference-limited multiple input multiple output cellular system," *Global Telecommunications Conference, 2000. GLOBECOM'00. IEEE*, 2000, pp. 1094-1096.

[12] Farooq Khan, *LTE for 4G Mobile Broadband: Aire Interface Technologies and Performance*, Cambridge University Press, 2009.

[13] 3GPP TS 21.101, "Technical Specifications and Technical Reports for a UTRAN-based 3GPP system (Release 9)", Dec. 2009.

[14] D. Wyner, "Shannon-theoretic approach to a Gaussian cellular multiple-access channel," *Information Theory, IEEE Transactions on,* vol. 40, pp.1713–1727, Nov. 1994.

[15] Ekram Hossain, Dong In Kim, Vijay K. Bharagave, *Cooperative Cellular Wireless Network,* Cambridge University Press, 2011.

[16] 3GPP TS 36.331, "E - UTRA Radio Resource Control (RRC) Protocol specification", Jun. 2010.

[17] 3GPP TS 23.203, "Policy and Charging Control Architecture," Mar. 2010.

[18] 3GPP TS 36.300, "EUTRA and EUTRAN Overall description", Sept. 2007.

[19] 3GPP TR 36.913, "Requirements for Further Advancements for Evolved Universal Terrestrial Radio Access (E-UTRA)," Dec. 2009.

[20] G. Boudreau, J. Panicker, N. Guo, R. Chang, N. Wang, and S. Vrzic, "Interference coordination and cancellation for 4G networks," *Communication. Magazine, IEEE,* vol. 47, no. 4, pp. 74–81, Apr. 2009.

[21] IEEE P802.16m/D2, "Local and Metropolitan Area Networks Part 16: Air Interface for Broadband Wireless Access Systems, Advanced Air Interface," Oct. 2009.

[22] Somekh and S. Shamai (Shitz), "Shannon-theoretic approach to a Gaussian cellular multiple-access channel with fading," *IEEE Information Theory*, *IEEE Transactions on* , vol. 46, no. 4, pp. 1401–1425, July 2000.

[23] S. Shamai (Shitz) and A. D. Wyner, "Information-theoretic considerations for symmetric, cellular, multiple-access fading channels—part I," *Information Theory*, *IEEE Transactions on* , vol. 43, no. 6, pp. 1877–1894, Nov. 1997

[24] 3GPP TR 25.813. "Radio interface protocol aspects (Release 7)," September 2006

[25] Borko Furht, Syed A. Ahson, *Long Term Evolution: 3GPP LTE Radio and Cellular Technology,* CRC Press, 2009.

[26] Huan Chen, Lei Huang, Sunil Kumar, *Radio resource management for multimedia QoS support in wireless networks,* Springer, 2004.

[27] M. H. Costa, "Writing on dirty paper," *Information Theory*, *IEEE Transactions on* ,vol. IT-29, no. 3, pp. 439–441, May 1983.

[28] Q.H. Spencer, C.B. Peel and A.L. Swindlehurst, "An introduction to the multi-user MIMO downlink," *Communications Magazine, IEEE* , vol.42, no.10, pp. 60- 67, Oct. 2004

[29] H. Shan, W. Zhuang, and Z. Wang, "Distributed cooperative MAC for multihop wireless networks," *Communication. Magazine*, *IEEE,* vol. 47, no. 2, pp. 126–133, Feb. 2009.

[30] P. Liu, Z. Tao, S. Narayanan, T. Korakis, and S. S. Panwar, "CoopMAC: a cooperative MAC for wireless LANs," *selected areas in Communications, IEEE Journal*, vol. 25, no. 2, pp. 340–354, Feb. 2007.

[31] T. E. Hunter and A. Nosratinia, "Diversity through coded cooperation," *Wireless Communications*, *IEEE Transactions on,* vol. 5, no. 2, pp. 283–289, Feb. 2006.

[32] A. Bletsas, H. Shin, M. Z. Win, and A. Lippman, "A simple cooperative diversity method based on network path selection," *Selected areas in communications, IEEE Journal,* vol. 24, no. 3, pp. 659–672, Mar. 2006.

[33] A.S. Ibrahim, A.K. Sadek, W. Su, and K. J. R. Liu, "Cooperative communications with relay-selection: when to cooperate and whom to cooperate with?" *Wireless Communications, IEEE Transactions on*, vol. 7, no. 7, pp. 2814–2827, Jul. 2008.

[34] J. Cai, X. Shen, J. W. Mark, and A. S. Alfa, "Semi-distributed user relaying algorithm for amplify-and-forward wireless relay networks," *Wireless Communications, IEEE Transactions on*, vol. 7, no. 4, pp. 1348–1357, Apr. 2008.

[35] A. S. Ibrahim, A. K. Sadek, W. Su, and K. J. R. Liu, "Cooperative communications with relay-selection: when to cooperate and whom to cooperate with?" *Wireless Communications, IEEE Transactions on,* vol. 7, no. 7, pp. 2814–2827, Jul. 2008.

[36] E Telatar, "Capacity of Multi-antenna Gaussian channels," *telecommunications, European transactions on*, vol. 10, 1999.

[37] S. Shamai and B. Zaidel, "Enhancing the cellular downlink capacity via co-processing at the transmitting end," *Vehicular Technology Conference, 2001. VTC 2001 Spring, IEEE*, pp. 1745–1749, May. 2001

[38] O. Somekh, Simeone, and M. Haimovich, "Distributed multi-cell zero-forcing beamforming in cellular downlink channels," *Global Telecommunications Conference, 2006. GLOBECOM '06. IEEE*, pp. 1-6, Nov. 2006.

[39] P. Zhang, X. Tao, J. Zhang and Y. Wang, "A vision from the future: beyond 3G TDD," *Communications Magazine, IEEE,* vol. 43, no. 1, pp. 38–44, Jan. 2005.

[40] Sergey Balandin, *next generation teletraffic and wired/wireless advanced networking,* Springer, 2008

[41] Howard huang, "MIMO communication for cellular networks", springer, 2012

[42] A.F. Molisch, "A generic model for MIMO wireless propagation channels in macro and microcells," *Signal Processing, IEEE Transactions on*, vol. 52, no. 1, pp. 61–71, Jan. 2004.

[43] L. M. Correia, *Mobile Broadband Multimedia Networks*. Elsevier, 2006

[44] T. M. Cover and J. A. Thomas, *Elements of Information Theory*. John Wiley and Sons Press, 1991

[45] E. Telatar, "Capacity of multi-antenna Gaussian channels," *Telecommunications, European Transactions on*, vol. 10, no. 6, pp. 585–596, Nov. 1996.

[46] D. Aktas, M.N. Bacha, J.S. Evans and Hanly, S.V.; , "Scaling results on the sum capacity of cellular networks with MIMO links," *Information Theory, IEEE Transactions on*, vol.52, no.7, pp. 3264- 3274, Jul. 2006.

[47] D.B. West, *Introduction to Graph Theory*. Prentice hall, 2001.

[48] R. Balakrishnan, K.Ranganathan,. *a textbook of graph theory*, Springer, 2000

[49] H. Christos, Papadimitriou, Kenneth Steiglitz, *Combinatorial optimization: algorithm and complexity*, Courier Dover Publications, 1998.

[50] Chisung Bae, Dong-Ho Cho, "Fairness-Aware Adaptive Resource Allocation Scheme in Multihop OFDMA System," *Communications Letters, IEEE,* Vol. 11, pp. 134-136, 2007.

[51] A.B. Carleial, "Interference channels," *Information Theory, IEEE Transactions on,* vol. IT-24, pp. 60-70, Jan. 1978.

[52] N. Al-Dhahir, "Overview and comparison of equalization schemes for space-time-coded signals with application to EDGE," *Signal Processing, IEEE Transactions on,* vol. 50, pp. 2477–2488, Oct. 2002.

[53] E. Biglieri, J. Proakis, and S. S. Shitz, "Fading channels: Information theoretic and communication aspects," *Information Theory, IEEE Transactions on,* vol. 44, pp. 2619–2692, Oct. 1998.

[54] H. Bolcskei, D. Gesbert, and A. J. Paulraj, "On the capacity of OFDMbased spatial multiplexing systems," *Communication, IEEE Transactions on*, vol. 50, pp.225–234, Feb. 2002.

[55] G. Caire and S. Shamai, "On the capacity of some channels with channel state information," *Information Theory, IEEE Transactions on*, vol. 45, pp. 2007–2019, Sept. 1999.

[56] C. Chuah, D. Tse, J. Kahn, and R. Valenzuela, "Capacity scaling in MIMO wireless systems under correlated fading," *Information Theory, IEEE Transactions on*, vol. 48, pp. 637–650, Mar. 2002.

[57] A. Goldsmith, S.A. Jafar, N. Jindal and S. Vishwanath., "Capacity limits of MIMO channels," *Selected areas in communications, IEEE Journals on*, vol.21, no.5, pp. 684- 702, Jun. 2003.

[58] Borko Furht, Syed A. Ahson, *Long Term Evolution: 3GPP LTE Radio and Cellular Technology,* CRC Press, 2009.

[59] 3GPP CR1002. "CDMA2000 Evaluation Methodology," Dec. 2004.

[60] 3GPP TR 25.813. " Radio interface protocol aspects (Release 7)," Sept. 2006.

[61] Huan Chen, Lei Huang, Sunil Kumar, *Radio resource management for multimedia QoS support in wireless networks,* Springer, 2004

[62] 3GPP R1-090725, "Setup of CoMP cooperation areas," Sept. 2009.

[63] 3GPP TR 25.996. "Multiple Input Multiple Output simulations," Jun. 2007.

[64] 3GPP R3-051138."Radio access architecture and interfaces, " Oct. 2005.

[65] 3GPP TS 21.101 "Technical Specifications and Technical Reports for a UTRAN-based 3GPP system (Release 9)," Sept. 2009.

[66] 3GPP TS 36.300. " overall Description Stage 2 (Release 10), " Jun. 2010.

[67] D.S. Baum, J. Hansen, J. Salo; "An interim channel model for beyond-3G systems: extending the 3GPP spatial channel model (SCM)," *Vehicular Technology Conference, 2005, VTC 2005-Spring. 2005, IEEE,* pp. 3132- 3136 May 2005.

[68] A. Saleh, and R.A. Valenzuela, , "A statistical model for indoor multi-path propagation," *Selected Areas in Communications, IEEE Journal on,* Vol. SAC-5, no. 2, pp. 128-137, Feb. 1987.

[69] L.M. Correia, *Wireless Flexible Personalized Communications, COST 259: European Cooperation in Mobile Radio Research,* New York Wiley Press, 2001.

[70] 3GPP TR 25.814. "evolved Universal Terrestrial Radio Access, " Sept. 2006.

[71] 3GPP R4-060270. “Micro cell scenario for initial or early evaluation of MIMO in EUTRA,” Feb. 2006.

[72] A. Goldsmith. *Wireless communications*, Cambridge University Press, 2005.

[73] M. Salem, A. Adinoyi and M. Rahman, “Fairness-aware radio resource management in downlink OFDMA cellular relay networks,” *wireless communications, IEEE transactions on,* Vol. 9, pp. 1628-1639, May 2010.

[74] S. Catreux, L.J. Greenstein and P.F. Dressen, “Simulation results for an interference-limited multiple-input multiple-output cellular system,” *Communications Letter, IEEE,* vol 4, pp. 334-336, Nov. 2000.

[75] O. Simeone, O. Somekh, H. V. Poor, and S. Shamai, “Local base station cooperation via finite-capacity links for the uplink of simple cellular networks,” *Information Theory, IEEE Transactions on,* vol. 55, no. 1, pp. 190-204, Jan. 2009.

[76] W. Jiang, Zhongzhao Zhang, “Base station cooperation based on location-aided incellular system,” *Electrical and Computer Engineering, CCECE’09*, pp. 157-160, May 2009.

[77] P. Liu, Z. Tao, Z. Lin, E. Erkip and S. Panwar, “Cooperative wireless communications: a cross-layer approach,” *Wireless Communications Magazine, IEEE,* vol. 13, no. 4, pp. 84-92, Aug. 2006.

[78] Peng Shang, Guangxi Zhu, Li Tan, Gang Su, “Transmit antenna selection for the distributed MIMO system,” *Networks Security, Wireless Communications and Trusted Computing, 2009. NSWCTC '09. International Conference on*, pp.449-453, Apr. 2009.

[79] W.Roh, A. Paulraj, "MIMO channel capacity for the distributed antenna systems," *Vehicular Technology Conference, 2002, Proceedings, VTC 2002-Fall, 2002 IEEE*, pp. 706- 709, Sept. 2002.

[80] V. Srinivasa, P. Nuggehalli, C. Chiasserini, "An analytical approach to the study of cooperation in wireless ad hoc networks," *Wireless Communications, IEEE Transactions on,* vol.4, no.2, pp. 722- 733, March 2005.

[81] 3GPP TR 136 913 V9.0.0, "LTE; Requirements for further advancements for evolved universal terrestrial radio access," Feb. 2010.

[82] S. Venkatesan, A. Lozano and R. Valenzuela, "Network MIMO: Overcoming intercell interference in indoor wireless systems," *Signals, Systems and Computers, 2007, ACSSC 2007, Conference Record of the Forty-First Asilomar Conference on*, pp.83-87, Nov. 2007.

[83] Q. Wang, "Application of BBU+RRU based CoMP system to LTE-Advanced," *Communications Workshops 2009, ICC Workshops 2009, IEEE International Conference on*, pp.1-5, 14-18 Jun. 2009.

[84] Zhaoyang Zhang, Jing Shi, Hsiao-Hwa Chen, "A cooperation strategy based on nash bargaining solution in cooperative relay network," *Vehicular Technology, IEEE Transactions on*, vol.57, no.4, pp.2570-2577, Jul. 2008.

[85] S. Venkatesan, "Coordinating base stations for greater uplink spectral efficiency in a cellular network," *Personal, Indoor and Mobile Radio Communications, 2007. PIMRC 2007. IEEE 18th International Symposium on*, pp.1-5, Sept. 2007.

[86] A.P. Maneki, "Honest functions and their application to the analysis of cryptographic protocols," *Computer Security Foundations Workshop, 1999. Proceedings of the 12th IEEE*, pp.83-89, 1999.

[87] C. Fragouli, E. Soljanin, "Information flow decomposition for network coding," *Information Theory, IEEE Transactions on*, vol.52, no.3, pp.829-848, Mar. 2006.

[88] Min Yang, Yuanyuan Yang, "A Hypergraph Approach to Linear Network Coding in Multicast Networks," *Parallel and distributed systems, IEEE transactions on,* vol.21, no.7, pp.968-982, Jul. 2010.

[89] J. Jeon, K. Son and Chong Song, "Spatial Resource Reuse in the Multi-Hop Cellular Networks: Difficulties and Benefits," *Global Telecommunications Conference, 2008. IEEE GLOBECOM 2008. IEEE*, pp.1-6, Nov. 2008.

[90] Lin Xiao, Laurie Cuthbert. "Improving Fairness in Relay-based Access Networks," in *Proceedings of the 11th international symposium on modeling, analysis and simulation of wireless and mobile system,* MSWiM'08, pp. 18-22, Nov. 2008.

[91] 3GPP R1-090613, "Discussions on CoMP SU-MIMO," Mar. 2009.

[92] 3GPP TR 36.819, "Coordinated multi-point operation," Dec. 2011.

[93] 3GPP R1-091903, "Adaptive Cell Clustering for CoMP in LTE-A," May. 2009.

[94] R.Y. Chang, Zhifeng Tao, Jinyun Zhang, "A Graph Approach to Dynamic Fractional Frequency Reuse (FFR) in Multi-Cell OFDMA Networks," *Communications, 2009. ICC '09. IEEE International Conference on*, pp.1-6, Jun. 2009.

[95] M. HU, J.S. Zhang, "Opportunistic Multi-Access: Multiuser Diversity, Relay-Aided Opportunistic Scheduling," *Mobile Networks and Applications,* Vol. 9, pp. 435–444, Nov. 2004.

[96] M. Kamoun, L. Mazet, "Base-Station Selection in Cooperative Single frequency cellular network," *Signal Processing Advances in Wireless Communications, 2007. SPAWC 2007. IEEE 8th Workshop on*, pp.1-5, Jun. 2007.

[97] Y. Chang, Z. Tao and J. Zhang, "A graph based approach to multi-cell OFDMA downlink resource allocation," *Global Telecommunications Conference, 2008. IEEE GLOBECOM 2008. IEEE*, pp.1-6, Nov. 2008.

[98] H. W. KUHN, "The Hungarian Method for the Assignment Problem," *Novel Research Logistics Quarterly,* Vol. 2, pp. 83-98, Mar. 1955.

[99] S. Gel'fand and M. Pinsker, "Coding for channels with random parameters," *Problem and Control Theory*, vol. 9, no. 1, pp. 19–31, 1980.

[100] T.S. Han and K. Kobayashi, "A new achievable rate region for the interference channel," *Information Theory, IEEE Transactions on,* vol. IT-27, pp. 49-60, Jan. 1981.

[101] N. Devroye, P. Mitran, and V. Tarokh, "Achievable rates in cognitive radio channels," *Information Theory, IEEE Transactions on,* vol. 52, pp. 1813-1827, May 2006.

[102] A. Jovi̇ći̇ć and P. Viswanath, "Cognitive radio: An information theoretic perspective," *Information Theory, IEEE transactions on,* vol.55, no.9, pp.3945-3958, Sept. 2009.

[103] W. Wu, S. Vishwanath, and A. Arapostathis, "Capacity of a class of cognitive radio channels Interference channels with degraded message sets," *Information Theory, IEEE Transactions on,* vol. 53, no. 11, pp. 4391-4399, Nov. 2007

[104] J. Jiang and Y. Xin, "On the achievable rate regions for interference channels with degraded message sets," *Information Theory, IEEE Transactions on,* vol. 54, pp. 4707-4712, Sept. 2008.

[105] Dae-Won Seo, S. Jeon, S. Chung, J. Kim, "Rate enhancement for the Gaussian Z-interference channel with transmitter cooperation," *Communications Letters, IEEE*, vol. 14, no. 9, pp 821-823, Sept. 2010.

[106] L. Zhou, W. Yu,"Gaussian Z-interference channel with a relay link: Achievable rate region and asymptotic sum capacity," *Information Theory, IEEE Transactions on,* vol.58, no.4, pp.2413-2426, Apr. 2012.

[107] H. Sato, "The capacity of the Gaussian interference channel under strong interference," *Information Theory, IEEE Transactions on,* vol. 27, no.6, pp. 786- 788, Nov. 1981.

[108] Wei Wu, S. Vishwanath, A. Arapostathis, "On the Capacity of Gaussian Weak Interference Channels with Degraded Message sets," *Information Sciences and Systems, 2006 40th Annual Conference on*, pp.1703,1708, 22-24 Mar. 2006.

[109] A. Jovicic, P. Viswanath, "Cognitive Radio: An Information-Theoretic Perspective," *Information Theory, 2006 IEEE International Symposium on*, pp.2413,2417, 9-14 Jul. 2006.

[110] Cao Yi, Chen Biao, Zhang Junshan, "A New Achievable Rate Region for Interference Channels with Common Information,"*Wireless Communications and Networking Conference, WCNC 2007. IEEE*, , pp.2069,2073, 11-15 Mar. 2007.

[111] Chong Hon-Fah, M. Motani, H.K. Garg, "Capacity Theorems for the "Z" Channel," *Information Theory, IEEE Transactions on*, vol.53, no.4, pp.1348,1365, Apr. 2007.

[112] I. Maric, R. Yates, and G. Kramer, "Capacity of interference channels with partial transmitter cooperation," *Information Theory, IEEE Transactions on,* vol.53, no.10, pp.3536-3548, Oct. 2007.

Appendix I

The method of definition of a code in interference channel with cooperation is similar to [101] Define an (n, K_{11}, K_{12}, K_{21}, K_{22}, ε) code for the modified IC with cooperative transmission model as a set of $K_{21}\cdot K_{22}$ codewords $x_2^n(i,j) \in \mathcal{X}_2^n$, and $K_{11}\cdot K_{12}\cdot K_{21}\cdot K_{22}$ codewords $x_1^n(i,j) \in \mathcal{X}_1^n$, $i \in \{1,2,\dots,K_{21}\}, j \in \{1,2,\dots,K_{22}\}, k \in \{1,2,\dots,K_{11}\}, l \in \{1,2,\dots,K_{12}\}$, such that the average probability of decoding error is less than ε . Call a quadruple (S_1, T_1, S_2, T_2) achievable if there exists a sequence of

$$(n, 2^{[nS_1]}, 2^{[nT_1]}, 2^{[nS_2]}, 2^{[nT_2]}, \varepsilon_n)$$

This definition allows the code such that $\varepsilon \to 0$ as $n \to \infty$. An achievable region for the modified IC with cooperative transmission model is the closure of a subset of the defined quadruple.

Define the time-sharing random variable Q to strictly extend the achievable region obtained using a convex hull operation, as in [100]. Thus, let $Q \in \mathcal{Q}$ be a time-sharing random variable whose n-sequences $q^n \triangleq (q^{(1)}, q^{(2)}, q^{(3)} \dots \dots q^{(n)})$ are generated independently of the messages, according to $\prod_{t=1}^{n} p(q^{(t)})$. The n-sequence w^n is given to both senders and both receivers. In the IC with transmitter cooperation model, the sender 2 generates its public and private message firstly, the messages of sender 2 encode to x_2. Due to the conferencing link between two senders, messages from sender 2 transmit to sender 1. Therefore, sender 1 can generate its own messages u_1 and v_1 separately. Then, messages of sender 1 encode to x_1. Considering an interference channel, the two receivers receive their own signal y_1, y_2 respectively. The mathematics are showed below

Encoding: To generate the codebook, first let $q^n \triangleq (q^{(1)}, q^{(2)}, q^{(3)} \dots \dots q^{(n)})$ be a sequence in Q^n chosen randomly according to $\prod_{t=1}^{n} p(q^{(t)})$, and known to the

senders and receivers. Considering the message exchange from sender2 to sender1, it has

$$p(u_1 \mid u_2, v_2, q) = \sum_{u_2 \in U_2, v_2 \in V_2} p(u_1 \mid u_2, v_2, q)\, p(u_2 \mid q)\, p(v_2 \mid q)\, p(q) \tag{1}$$

$$p(v_1 \mid u_2, v_2, q) = \sum_{u_2 \in U_2, v_2 \in V_2} p(v_1 \mid u_2, v_2, q)\, p(u_2 \mid q)\, p(v_2 \mid q)\, p(q) \tag{2}$$

As described in (1), for a give time variable q, the system generate message for sender 2 firstly, and transmit the message to sender 1 in order to assist sender 1 generate its own message. (11), (12) show the distribution of the described procedure.

Then the codebook can be generated according to the distribution mentioned in (1)

Define the message index spaces as follow

$$\begin{aligned} S_{11} &:= \{1, 2, \ldots, 2^{[n(S_1 - \varepsilon)]}\} \\ S_{12} &:= \{1, 2, \ldots, 2^{[n(T_1 - \varepsilon)]}\} \\ S_{21} &:= \{1, 2, \ldots, 2^{[n(T_2 - \varepsilon)]}\} \\ S_{22} &:= \{1, 2, \ldots, 2^{[n(S_2 - \varepsilon)]}\} \end{aligned} \tag{3}$$

Therefore, it can send a four dimensional message.

$$s := (s_{11}, s_{12}, s_{21}, s_{22}) \in S := S_{11} \times S_{12} \times S_{21} \times S_{22} \tag{4}$$

The definition used here (16), (17) are strictly following in [101]

If the probability of error could be arbitrarily small under such a message, the rates achieved will be (S_1,T_1,S_2,T_2) for the sender-receiver pairs $Tx_1 \rightarrow Rx_1$, $Tx_1 \rightarrow Rx_2$, $Tx_2 \rightarrow Rx_2$, $Tx_2 \rightarrow (Rx_1, Rx_2)$, respectively.

Recall that the messages actually sent over the IC with transmitter cooperation are elements of $\mathcal{X}_1^n, \mathcal{X}_2^n$ (u,v are modified message which are used to assist the proof, but for realistic IC case, only $\mathcal{X}_1^n, \mathcal{X}_2^n$ transmit from sender 1 and sender 2

respectively). The messages are mapped into the single space $\mathcal{X}_2^n$ as follow.

i) To send s_{21} and s_{22}, look up the sequences $u_2^n(s_{22})$ and $v_2^n(s_{21})$.

ii) Generate x_2^n i.i.d. according to $\prod_{t=1}^{n} p(x_2^{(t)} \mid u_2^n(s_{22}), v_2^n(s_{21}), q^n)$ and send.

The information exchange during the two transmitters is as follows. From x_2^n being generated, S_1 receives the exchanged information and can recover u_2^n and v_2^n. According to the Shannon Theorem, (5)-(10) ensure the recovery is indeed possible. Then the new messages (s_{11},s_{12}) is encoded.

S_1 proceeds as follows.

i) To send s_{11} and s_{12}, look up the sequences u_1^n and v_1^n such that $(u_1^n, u_2^n, v_2^n, q^n)$ and $(v_1^n, u_2^n, v_2^n, q^n)$ are jointly typical tuples respectively.

ii) Generate x_1^n i.i.d. according to $\prod_{t=1}^{n} p(x_1^{(t)} \mid u_1^n, v_1^n, q^n)$ and send.

To be generals, the distribution of encoding can be derived as follow.

Let $Z := (Y_1, Y_2, X_1, X_2, U_1, V_2, U_1, V_2, Q,)$, and let $\mathcal{P}$ be the set of distribution on Z that can be decomposed into the form

$$\begin{aligned} & p(q)\,p(u_2 \mid q)\,p(v_2 \mid q)\,p(x_2 \mid u_2, v_2, q) \\ & \times p(u_1 \mid u_2, v_2, q)\,p(v_1 \mid u_2, v_2, q)\,p(x_1 \mid u_1, v_1, q) \\ & \times p(y_1 \mid x_1, x_2)\,p(y_2 \mid x_1, x_2) \end{aligned} \tag{5}$$

Decoding: it is noted that the two receivers are decoded independently. For receiver 1, only two messages need to recover, which are private message from sender 1 s_{11} and public message from sender 2 s_{21}. Therefore, a two dimension decoding function are derived, where ψ_1^{11} indicates the function of decoding private message s_{11} and , ψ_1^{21} indicates the function of decoding public message s_{21}.

$$\psi_1: \mathcal{Y}_1^n \times Q^n \to S_{11} \times S_{21}$$
$$\psi_1(y_1^n, q^n) = \left(\psi_1^{11}(y_1^n, q^n), \psi_1^{21}(y_1^n, q^n)\right) \tag{6}$$

For receiver 2, considering the characteristic of cooperation, not only the private message s_{22} and public message s_{21} from sender 2 need to recover, but also the cooperative message s_{12} from sender 1 needs to recover. Therefore, a three dimension decoding function are shows as follow, where ψ_1^{12} indicates the function of decoding cooperative message s_{12} , ψ_1^{21} indicates the function of decoding message s_{21} and , ψ_1^{22} indicates the function of decoding private message s_{21}.

$$\psi_2: \mathcal{Y}_2^n \times Q^n \to S_{12} \times S_{21} \times S_{22}$$
$$\psi_2(y_2^n, q^n) = \left(\psi_2^{12}(y_2^n, q^n), \psi_2^{21}(y_2^n, q^n), \psi_2^{22}(y_2^n, q^n)\right) \tag{7}$$

Considering the message s_{11}, s_{12}, s_{21} and s_{22} are all modified messages; only messages x_1 and x_2 would be received at the receiver in a realistic IC with transmitter cooperation model. The inputs x_1^n, x_2^n are received at Rx_1, Rx_2 as y_1^n, y_2^n according to the conditional distributions

$$p^n(y_1^n \mid x_1^n, x_2^n) = \prod_{t=1}^{n} p(y_1^{(t)} \mid x_1^{(t)}, x_2^{(t)}) \tag{8}$$

$$p^n(y_2^n \mid x_1^n, x_2^n) = \prod_{t=1}^{n} p(y_2^{(t)} \mid x_1^{(t)}, x_2^{(t)}) \tag{9}$$

Appendix II

Considering a memoryless Gaussian channel scenario, the received signals in "standard" form [106] for IC with transmitter cooperation is given by

$$\begin{aligned} Y_1 &= X_1 + \sqrt{a_{21}} X_2 + Z_1 \\ Y_2 &= \sqrt{b_{12}} X_1 + X_2 + Z_2 \end{aligned} \tag{1}$$

Where X_1, X_2 are the transmit signals with transmit power constraints P_1 and P_2 respectively, a_{21} and b_{12} are real numbers, and Z_1 and Z_2 are independent AWGN with zero means and variance N_1, N_2, respectively.

To simplify the notation, let $\gamma(x) = \frac{1}{2}\log_2(1+x)$. Let Q, the time-sharing random variable, be constant. Define $\alpha, \beta \in \mathbb{R}$, and $\alpha, \bar{\alpha}, \beta, \bar{\beta} \in [0,1]$ with $\alpha + \bar{\alpha} = 1$, $\beta + \bar{\beta} = 1$. Therefore, independent Gaussian codebooks of sizes $2^{nS_1}, 2^{nT_1}, 2^{nS_2}$ and 2^{nT_2} are generated according to i.i.d. Gaussian distributions $U_1 \sim N(0, \alpha P_1)$, $V_1 \sim N(0, \bar{\alpha} P_1)$, $U_2 \sim N(0, \beta P_1)$ and $V_2 \sim N(0, \bar{\beta} P_1)$ respectively.

At receiver 1, (U_1, V_2) are decoded at Rx_1 as U_2 is treated as noise. Since each mutual-information bound can be expanded in terms of entropies, the set of achievable rates (S_1, T_2) denoted here by C_1 is given by

$$\begin{cases} S_1 \le \gamma\left(\dfrac{\alpha P_1}{N_1 + a_{21}\beta P_2}\right) \\ T_2 \le \gamma\left(\dfrac{a_{21}\bar{\beta} P_2}{N_1 + a_{21}\beta P_2}\right) \\ S_1 + T_2 \le \gamma\left(\dfrac{\alpha P_1 + a_{21}\bar{\beta} P_2}{N_1 + a_{21}\beta P_2}\right) \end{cases} \tag{2}$$

At receiver 2, (U_2, V_1, V_2) are decoded at Rx_2 as U_1 is treated as noise. This is a multiple-access channel with a rate-limited link at the transmitter, which has complete knowledge of Tx_2. This channel is a special case of the multiple access relay

channel studied in [106]. The set of achievable rates is (S_2, T_1, T_2), denoted by C_2, where

$$\begin{cases} S_2 \le \gamma(\dfrac{\beta P_2}{N_2 + b_{12}\alpha P_1}) \\ T_1 \le \gamma(\dfrac{b_{12}\bar{\alpha} P_1}{N_2 + b_{12}\alpha P_1}) + R_0 \\ T_2 \le \gamma(\dfrac{\bar{\beta} P_2}{N_2 + b_{12}\alpha P_1}) \\ S_2 + T_1 \le \gamma(\dfrac{b_{12}\bar{\alpha} P_1 + \beta P_2}{N_2 + b_{12}\alpha P_1}) + R_0 \\ S_2 + T_1 + T_2 \le \gamma(\dfrac{b_{12}\bar{\alpha} P_1 + P_2}{N_2 + b_{12}\alpha P_1}) + R_0 \end{cases} \tag{3}$$

An achievable rate region of the IC with transmitter cooperation is then the set of all (R_1, R_2) such that $R_1=S_1$ and $R_2=S_2+T_1+T_2$ for some $(S_1, T_2) \in C_1$ and $(S_2, T_1, T_2) \in C_2$. Furthermore, since C_1 and C_2 depend on the power allocation splitting ratio α, β, the convex hull of the union of all such (R_1, R_2) sets over all choices of α, β are achievable.

It is possible to use a Fourier-Motzkin elimination to verify the achievable rate region for arbitrary parameter value α, β, the achievable (R_1, R_2) being formed.

$$R_{\alpha,\beta} = \left\{ (R_1, R_2) \left| \begin{array}{c} R_1 \le \gamma(\dfrac{\alpha P_1}{N_1 + a_{21}\beta P_2}) \\ R_2 \le \min\{\gamma(\dfrac{b_{12}\bar{\alpha} P_1 + P_2}{N_2 + b_{12}\alpha P_1}) + R_0, \\ \gamma(\dfrac{a_{21}\bar{\beta} P_2}{N_1 + a_{21}\beta P_2}) + \gamma(\dfrac{b_{12}\bar{\alpha} P_1 + \beta P_2}{N_2 + b_{12}\alpha P_1}) + R_0\} \\ R_1 + R_2 \le \gamma(\dfrac{\alpha P_1 + a_{21}\bar{\beta} P_2}{N_1 + a_{21}\beta P_2}) + \gamma(\dfrac{b_{12}\bar{\alpha} P_1 + \beta P_2}{N_2 + b_{12}\alpha P_1}) + R_0 \end{array} \right. \right\} \tag{4}$$

The convex hull of the union of the rate region over arbitrary α and β gives the complete achievability region. Since the union of the rate region, i.e. $\cup_{0<\alpha,\beta<1} R_{\alpha,\beta}$, is convex, the convex hull is not needed. This is proved below.

Consider the regime where a_{21}, $b_{12}<1$, i.e., in weak interference and weak cooperation scenario. In this case, the constraint $R_2 \le \gamma\left(\frac{b_{12}\bar{\alpha} P_1 + P_2}{N_2 + b_{12}\alpha P_1}\right) + R_0$ is ignored. Then the

achievable rate region can be represented in a more compact form as follows.

$$R_{\alpha,\beta} = \left\{ (R_1, R_2) \middle| \begin{array}{c} R_1 \le f_1(\alpha,\beta) \\ R_2 \le f_2(\alpha,\beta) \\ R_1 + R_2 \le f_3(\alpha,\beta) \end{array} \right\} \tag{5}$$

Where

$$\begin{aligned} f_1(\alpha,\beta) &= \gamma\left(\frac{\alpha P_1}{N_1 + a_{21}\beta P_2}\right) \\ f_2(\alpha,\beta) &= \gamma\left(\frac{a_{21}\bar{\beta} P_2}{N_1 + a_{21}\beta P_2}\right) + \gamma\left(\frac{b_{12}\bar{\alpha} P_1 + \beta P_2}{N_2 + b_{12}\alpha P_1}\right) + R_0 \\ f_3(\alpha,\beta) &= \gamma\left(\frac{\alpha P_1 + a_{21}\bar{\beta} P_2}{N_1 + a_{21}\beta P_2}\right) + \gamma\left(\frac{b_{12}\bar{\alpha} P_1 + \beta P_2}{N_2 + b_{12}\alpha P_1}\right) + R_0 \end{aligned} \tag{6}$$

To verify the union of rate region pentagons, it is easy to prove $f_1(\alpha,\beta), f_2(\alpha,\beta)$ and $f_3(\alpha,\beta)$ are all continuous functions of α,β, as α,β are from 0 to 1. When α increases from 0 to 1, $f_1(\alpha,\beta)$ is monotonically increasing and both $f_2(\alpha,\beta)$ and $f_3(\alpha,\beta)$ are monotonically decreasing. On the other hand, when β increases from 0 to 1, $f_1(\alpha,\beta)$, $f_3(\alpha,\beta)$ are monotonically decreasing, while $f_2(\alpha,\beta)$ is increasing. Therefore, as shown in Figure 3, the upper left corner point moves downward in the R_1-R_2 plane as α increases. Moreover, the lower right corner point moves downward and to the right as α increases and β decreases. Consequently, the union of theses expanded pentagons is defined by $R_1 \le \left(\frac{P_1}{N_1}\right)$, $R_2 \le \left(\frac{b_{12}P_1+P_2}{N_2}\right) + R_0$, and the lower-right corner points of the pentagons (R_1,R_2) with

$$\begin{cases} R_1 = \gamma\left(\dfrac{\alpha P_1}{N_1 + a_{21}\beta P_2}\right) \\ R_2 = \gamma\left(\dfrac{b_{12}\bar{\alpha} P_1 + \beta P_2}{N_2 + b_{12}\alpha P_1}\right) + \gamma\left(\dfrac{a_{21}\bar{\beta} P_2}{N_1 + a_{21}\beta P_2 + \alpha P_1}\right) + R_0 \end{cases} \tag{7}$$

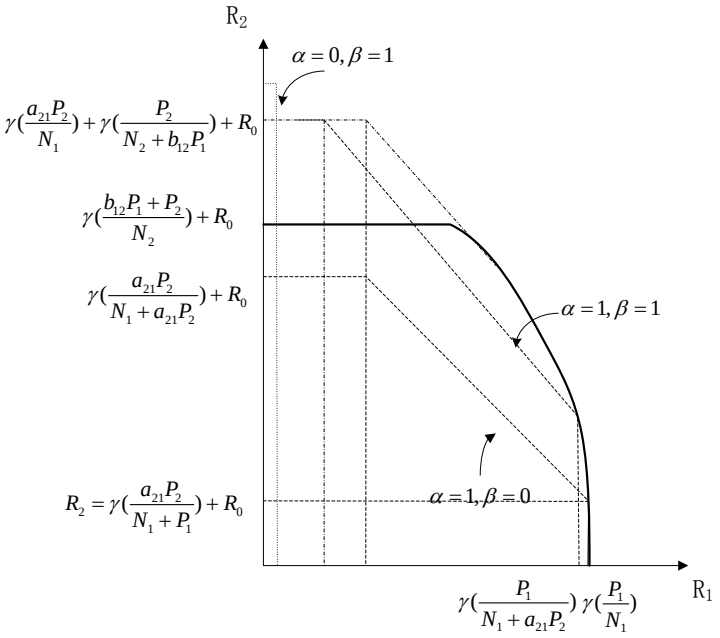

Figure 1 Union of rate region pentagons in weak interference scenario

To prove the convexity of the region, α, β is derived in terms of R_1 and substituted into the expression for R_2 in (7), giving R_2 as a function of R_1:

$$R_2 = \xi + \gamma(\eta 2^{-2R_1}) \tag{8}$$

Where $\xi = \gamma(\frac{b_{12}\bar{\alpha}P_1 + \beta P_2}{N_2 + b_{12}\alpha P_1})$, $\eta = \frac{a_{21}\bar{\beta}P}{N_1 + a_{21}\beta P_2}$.

Observe from (8) that R_2 is a continuous function of R_1 from 0 to $\gamma(\frac{P_1}{N_1})$. Now, taking the first and second order derivatives of R_2 with respect to R_1 in (8)gives

$$R_2^{'} = \frac{-\eta}{2^{2R_1} + \eta}, \; R_2^{''} = -\frac{2\eta \cdot \ln(2) \cdot 2^{2R_1}}{(2^{2R_1} + \eta)^2} \tag{9}$$

Since $\eta > 0$, $R_2' \leq 0$ and $R_2'' \geq 0$. As a result, the curve (7) is concave. Therefore, in the weak interference regime where a_{21}, $b_{12}<1$, the rate region is convex so that the convex hull is not needed. Thus the achievable rate region simplifies to

$$\begin{cases} R_1 \le \gamma(\dfrac{\alpha P_1}{N_1 + a_{21}\beta P_2}) \\ R_2 \le \min\{\gamma(\dfrac{b_{12}P_1 + P_2}{N_2}) + R_0, \gamma(\dfrac{b_{12}\bar{\alpha}P_1 + \beta P_2}{N_2 + b_{12}\alpha P_1}) + \gamma(\dfrac{a_{21}\bar{\beta}P_2}{N_1 + a_{21}\beta P_2 + \alpha P_1}) + R_0\} \end{cases} \quad (10)$$

Now, consider the strong interference and strong cooperation scenario where a_{21}, $b_{12}>1$. In this regime, as α, β are increase from 0 to 1, $f_1(\alpha, \beta)$ is monotonically increasing and both $f_2(\alpha, \beta)$ and $f_3(\alpha, \beta)$ are monotonically decreasing. Therefore, using similar techniques, it can be proved that the convex hull is not needed. Thus, the achievable rate region simplifies to

$$\begin{cases} R_1 \le \gamma(\dfrac{P_1}{N_1}) \\ R_2 \le \gamma(\dfrac{b_{12}P_1 + P_2}{N_2}) + R_0 \\ R_1 + R_2 \le \gamma(\dfrac{a_{21}P_2}{N_1}) + \gamma(\dfrac{b_{12}P_1}{N_2}) + R_0 \end{cases} \quad (11)$$

This derivation has given achievable rate regions for regimes a_{21}, $b_{12}<1$ and a_{21}, $b_{12}>1$ as in (6.1) and (6.2) respectively.